Rebuttal ACPD

BOLD = reviewer comment
Italic = answer to reviewer comment
Red = highlighted changes in manuscript

Comments previously provided by a reviewer

(Editor: These comments have not been addressed in this ACPD version and thus need to be addressed in this round of review.)

I am afraid that even after reading the article, I do not understand why the authors choose to explain air quality over Paris based on meteorology at the SIRTA location, when regional and local emissions and atmospheric transformations during long range transport are the major drivers of ambient pollution. These major drivers are mentioned towards the end as future work, but studies should start there. For example, even if MLH or wind speed is low, zero emissions = no air pollution.

Answer:
Thank you for this comment.
Indeed we do not inted to explain Paris air quality using the SIRTA site - the focus is on air quality at the SIRTA site, which is near Paris and representative of suburban background concentrations. We have clarified this in the manuscript (see changes in L11, L88, L94, L127, L234, L502). The aim of this study is to quantify how meteorological factors influence pollutant concentrations and thus add to system understanding. It has been shown in previous studies that pollutant concentrations are not solely driven by emissions, and can be exacerbated or weakened substantially by certain meteorological conditions. For SIRTA, this has been described for example by Dupont et al., 2016.
It was not intended to set up a prognostic model to forecast PM1 as accurately as possible in time.
Emissions of pollutants or precursor gases undoubtedly constitute a prerequisite to air pollution, but pollutant concentrations are not solely driven by anthropogenic emissions, but strongly affected by varying amounts of natural background emissions (see e.g., Liora et al., 2016, DOI: 10.1016/j.atmosenv.2016.04.040, Jiang et al. 2019, DOI: 10.5194/acp-19-15247-2019). Thus, high concentrations of particulates could also occur

during episodes with low anthropogenic emissions. This is particularly the case in summer, when biogenic organic emissions are high (this is mentioned in the introduction, L56).
The influence of meteorology can lead to quite different air pollution situations, even if emissions are constant. In winter, meteorological conditions exert great influence on formation pathways, as we describe in chapter 4.2.1. For example, condensation of ammonium nitrate in the aerosol phase is enhanced at low ambient temperatures and high relative humidity (see e.g., Pay et al., 2012; Bressi et al., 2013; Petetin et al., 2014; Petit et al., 2015). Hence, even if emissions would be not above average levels, this formation mechanism would increase the concentrations of pollutants.
Transformation processes are partly covered by meteorological parameters, e.g., through the influence of temperature (please see also answers to Referee #3 comments). Obviously, the model does still not capture all of the occurring variance of PM1 concentrations, but since it was not the intention to set up a predictive framework, the focus is not primarily on accuracy, but on interpretability. Hence, the included parameters are deemed adequate for the analysis
In the updated version of the manuscript, we have taken great care to consider this comment and now more clearly communicate the main goal of this manuscript:

- *L3: However, the scientific understanding of the ways by which complex interactions of meteorological factors lead to high pollution episodes is inconclusive, as the effects of meteorological variables are not easy to separate and quantify*
- *L6: In this study, a novel, data-driven approach based on empirical relationships is used to characterise, quantify and better understand the meteorology-driven component of PM1 variability.*
- *L8: Changed to "Based on the model, an isolation and quantification of individual meteorological influences for process understanding is achieved using SHapley Additive exPlanation (SHAP) regression values.*
- *L87: Changed to "Here, the multivariate and highly interconnected nature of the processes determining local PM1 concentrations is analysed in a data-driven way. Therefore, a state-of-the-art explainable machine learning model is set up to reproduce the variability of PM1 concentrations, thereby capturing empirical relationships between PM1 concentrations and meteorological parameters. The goal is to separate and quantify influences of the meteorological variables on PM1 concentrations to advance the process understanding of the complex mechanisms that govern pollution concentrations at the measurement site."*

The authors frame it as "we should take atmospheric and environmental processes into account during the development of efficient pollution

mitigation strategies"/"a basis for future clean air programs", but AirParif can't exactly change wind conditions or MLH orT/RH.

These statements were aimed to show the potential benefits of considering atmospheric and environmental conditions when future measures to prevent air pollution are discussed. This relates mainly to three points:

- *a) A realistic assessment of the effectiveness of measures against air pollution needs to take atmospheric and environmental processes into account as these processes partly control its variability. For example, if changes in PM concentrations due to traffic restrictions were to be determined, a simple comparison of pre-restriction and post-restriction concentrations would not be sufficient, as meteorological influences would be omitted. Machine learning approaches can be very useful to characterize the efficiency of mitigation policies. Recent lockdown in Spain is an adequate example here (Petetin et al., 2020, DOI: https://doi.org/10.5194/acp-20-11119-2020)*
- *b) Weather conditions which exacerbate pollutant concentrations are identified using the SHAP framework. On this basis, air-pollution measures could be adjusted depending on expected meteorological conditions. For example, warnings could be expressed to the public to remain vigilant or stay at home if possible.*
- *c) In a changing climate, more unfavorable meteorology could trigger and/or exacerbate PM pollution episodes, lowering the role of emission restrictions.*

To make this clearer in the manuscript, the following changes were made:

- *L47: The sentence "It is therefore crucial to take atmospheric and environmental processes into account during the development of efficient pollution mitigation strategies" was removed .*
- *The explanation relating to future clean air program was shifted to the end of the introduction and expanded; L96-106 now read:*
  "... allowing to infer meteorology-dependent processes driving PM concentrations at high temporal resolution.. Typical situations that lead to high PM1 concentrations are identified, serving as a decision support to policymakers to issue preventative warnings to the public if these situations are to be expected. In addition, by directly accounting for meteorological effects on PM1 concentrations, such a machine learning-based framework could help in assessing the effectiveness of measures towards better air quality. Furthermore, the proposed ML framework can be viewed as a first step towards a data-driven, prognostic tool in operational air quality forecasting, complementary to CTM approaches.

Maybe this can be used to forecast periods of bad air quality - but they describe some important events that the model fails to reproduce because it is missing major drivers in the inputs (lines 390, 426-427).

We show several examples where the model is well able to reproduce episodes of high pollutant concentrations (sections 4.4.1-4.4.3). This is encouraging and shows the appropriateness of the approach. There are of course also situations in which the model fails to reproduce high-pollution situations. These situations are shown in detail to stimulate further research in this direction.
As stated earlier, the current model setup was chosen for the purpose of improving the understanding of how meteorological factors influence pollutant concentrations, and to quantify potential influences (which was more clearly stated in L87-105). Setting up a probabilistic forecast model based on top of the presented framework would undoubtedly require many adjustments to include the factors correctly pointed out by the referee..

So I am not sure this study is an advance over previous knowledge.
Extensive changes were made to the manuscript to emphasize new scientific insights (see previous answers and answers to Referee#3 comments)

Anonymous Referee #1

The research work employs field measurements of Particulate Matter smaller than1μm in diameter (PM1), routine meteorology data and propose a machine learning framework in air-pollution forecasting. The authors address the significant challenge of Interpretability in machine learning using the SHapley Additive exPlanation (SHAP)regression values.

A general comment is related to the aim of the proposed work. Although the role of meteorology on PM concentrations is well studied, the paper proposes a novel method/tool of explainable machine learning in atmospheric sciences. The results support the use of explainable machine learning as a statistical modeling framework in operational air quality forecasting. The authors comment on this in the conclusion section but could highlight the ability of the proposed framework earlier in the manuscript.

Thank you for your assessment.
In order to highlight the capability of the framework in air quality forecasting, the

following statement was added to the introduction (L102): "Furthermore, the proposed ML framework can be viewed as a first step towards a data-driven, prognostic tool in operational air quality forecasting, complementary to CTM approaches.."

While the results of the study are of local interest the proposed modelling framework has a high replication potential in areas with limited PM1 field measurements and therefore has a general implication in atmospheric science. Some concern is related to the use of meteorological data for the period of July to mid-November 2016. It is useful to include some descriptive statistical analysis of the meteorological data for all sites in order to compare and highlight the suitability of using meteorological data from the Paris Charles de Gaulle Airport.
Please note that only MLH was substituted during that time, all the other variables were not affected by the instrument failure.
An appendix was added. Figs A1 and A2 now provide a comparison of MLHs measured at Sirta vs. MLH measured at Charles de Gaulle airport for available data of the year 2016.

Furthermore, the locations of all measurement sites should be included in the map of the area of study and use more appropriate location mark labels.
Map (Figure 1) was changed accordingly.

The authors could provide some descriptive statistical analysis of the PM1 field mea-surements. This analysis could provide thresholds of high-pollution events in the region(e.g. similar to the >95 percentiles used in the paper).
Table showing mean, interquartile range, 95 percentile was added in section 4.3
Several thresholds were tested to define high-pollution events (e.g., >75%, >90%, >95%). It was found that the more extreme the events, the clearer the meteorological influence, which points to a relatively narrow set of meteorological characteristics responsible for high-pollution events. The decision to finally use the 95th percentile for the analysis was because this is a typical threshold for extreme value analysis. Below is shown the plot for extreme events >75th percentile; patterns are similar, but less distinct compared to >95th percentile as shown in the manuscript.

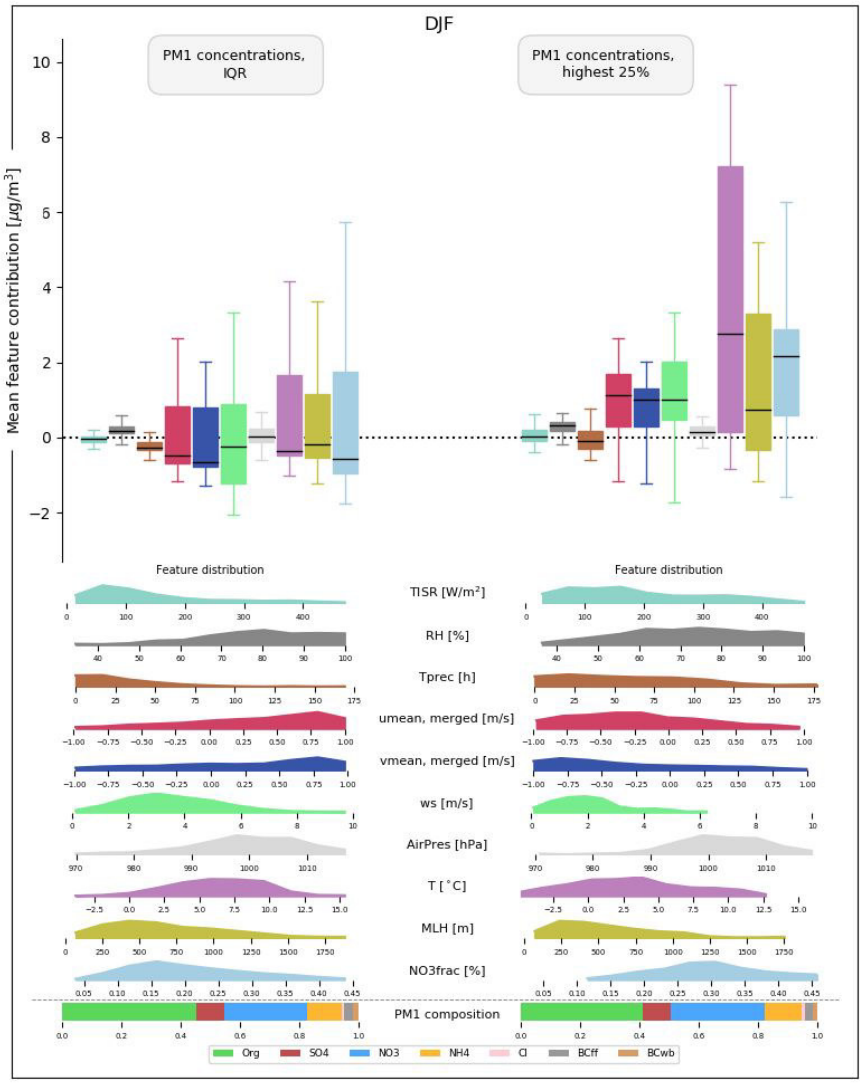

Please note that a more extensive description of the statistics of the PM1 field measurements is also provided in Petit et al., 2014 (DOI: https://doi.org/10.5194/acp-14-13773-2014), Petit et al., 2015 (DOI: https://doi.org/10.5194/acp-15-2985-2015), Petit et al., 2017 (DOI: https://doi.org/10.1016/j.atmosenv.2017.02.012)

The overall ability of the proposed framework could be also evaluated using exceedances forecast verification metrics (e.g. Probability of Detection, False Alarm Ratio etc.) for certain PM1 thresholds. This analysis could be complementary to the analysis of high-pollution case-studies and role of meteorological conditions of high-pollution events.

As the main objective of this study is to advance the understanding of meteorological drivers, a regression model was set up and validated to reproduce the temporal development of PM concentrations. The model that was set up for this task does not do a classification, therefore calculating the Probability of Detection or False Alarm Rate might not be suitable for validation. Hence, while these are certainly good suggestions for a classification framework, they are out of the scope of the manuscript and could be included in future work on this topic.

The paper presentation and structure is clear and supports the discussion of the results. The authors give proper credit to earlier published work and discuss their findings appropriately. The figures in the manuscript support the discussion of the results.
Thank you!

In Figures 9 and 10 the color-bar of the PM1 composition could be misleading. It is advised to change to avoid confusion with the feature contributions color scales.
The colors used for major PM1 species are consistent with previous literature (e.g., Petit et al. 2014, Petit et al. 2015, Dupont et al. 2016), so the colors of the meteorological variables were changed instead. In addition, a horizontal line was added to more clearly separate the PM1 composition plot.

The authors should also check of consistency of abbreviations throughout the manuscript. For example, Mixed-layer height (MLH) in some figures is abbreviated as BLH.
Thank you, BLH was changed to MLH in all affected plots.

Anonymous Referee #3

This paper presents a machine-learning built model approach to analyse an extensive multi-parameter dataset at observational in a suburban area south of Paris. The focus of the manuscript is using a recently published tool ("SHapley Additive exPlanation(SHAP) values") to analyse the machine-learning model's predictions and then attribute drives of the statistical model.

The paper presents large amounts of information about the output from the analysis tool, but not enough focused justification or evidence is presented

about how novel these interpretations are or how that they could be used for air pollution mitigation policy etc. At points, the paper even reads as if the authors are suggesting that authorities seek to mitigation against the meteorology contribution to air pollution. Could this analysis be used to make a forecasting tool if parameters were gained in real-time? If so,how long ahead would these predictions be expected to be useful for? Would this be useful in a public health context?

Thank you for your assessment.

The focus of this study is not on the prediction of pollutant concentrations in time, but to contribute to the advancement of the scientific understanding of how meteorology influences air pollution. The machine-learning framework presented in this study provides observation-based, quantitative estimations for the influence of various meteorological factors to PM1 at the same time, enabling their direct comparison. The model does allow for interactions between the meteorological factors, and on this basis, a separation and comparison of meteorological influences on any individual event is feasible. This is a novel aspect, as it allows to extract empirical patterns from the data set that are hard to detect using established statistical methods.

Setting up a forecasting tool is a possible extension of the machine-learning framework established within this study, but not the key objective here. This is why we only outline such possible applications and their usefulness at the end of the manuscript. So no, our analysis framework in its present form is not intended as a forecasting tool, and cannot be converted into one without more work. Hence, the reliability of such a forecast tool was not assessed. It is likely that the PM forecast would greatly depend on the reliability of the forecasted meteorological conditions. In its present configuration, however, our tool can determine an 'expected' level of air pollution under given meteorological conditions. By comparing this to actual observations, the effect of any source reductions (e.g. via policies) can be assessed. These points were added in L510-520.

The following specific changes were made in the manuscript:

- *L2 & 3: "substantially contribute to" was changed to "substantially influence". The wording "contribute to" might indeed be misleading here, as it could sound as if meteorology actively emits pollutants.*
- *Throughout the manuscript, the wording "meteorological contribution" was changed to "meteorological influence" or removed, if not referring to the ML model (caption chapters 4.2, 4.2.1-4.2.4, L265, L294, L295, 295, 303, 317, 329, 361, 362, 376, 424, 461, 483, 486)*

- *L46: the sentence "It is therefore crucial to take atmospheric and environmental processes into account during the development of efficient pollution mitigation strategies" was removed. This point is now made clearer at the end of the introduction*
- *See changes in lines 80-85; the goal of the study is now stated more precisely and benefits in a public health context are described*
- *L476-479: ...As interactions between the meteorological variables are accounted for, the model enables the separation, quantification and comparison of their respective impacts the individual events. It is shown that ambient meteorology can substantially exacerbate air pollution. Results of this study point to a distinguished role of shallow MLHs, low temperatures and low wind speeds during peak PM1 concentrations in winter*
- *L512-515: changed to "For policy makers, the presented approach could prove beneficial in multiple ways and serve as a decision aid for air policy measures. Preventative warnings could be issued to the public if the identified meteorological conditions exacerbating air pollution are to be expected. Another application would be to attribute changes in air quality to policy measures by comparing an 'expected' level of air pollution under given meteorological conditions to actual observations (e.g., Cermak2009 and Knutti 2009), which may help…"*

A core premise (in the abstract and elsewhere) is that we do not fully understand the contribution of meteorology to high air pollution episodes is true, however, this does justify the framework used here which omits two other key drivers (chemistry and emis-sions). Apart from a few mentions, it is not clear how are these contributions and con-sidered in this method. Are the contributions of these processes just assumed to be part of the meteorological contributions? This needs to be a lot clearer.

The focus of this paper explicitly lies on the analysis of the influence of meteorological conditions on PM1 concentrations. We are fully aware that meteorology alone cannot explain PM1; one of our aims is to ultimately be able to 'remove' the effect of meteorology, and retain the effects of emissions (and to a lesser degree, chemistry), which to some extent can be influenced directly by policy (this was added in L99-102). As mentioned in other answers above, pollutant concentrations have been shown to be exacerbated or decreased by certain meteorological conditions (e.g., Dupont et al., 2016). It is shown that the model is able to capture a large fraction of the occurring variation of daily PM1 concentrations, which shows that the variables chosen as inputs are indeed important drivers. Even without

explicitly considering emissions and chemistry, the model explains between 50-60% of the day-to-day PM1 variability. Thus, for the location and data set analysed here, the influence of meteorological variability on PM1 is at least as large as the influence of the variability of emissions and chemistry. Hence, given the key objective of this study, the presented framework is suitable for the analysis by capturing key meteorology-based processes. The detailed analysis presented in chapter 4.4 emphasizes that the temporal trends of PM1 concentrations are largely well captured.
Some of the meteorological parameters inherently contain information on chemistry and emissions. For example, RH, solar radiation, and temperature can influence local transformation processes, as detailed in L44-60. Temperature also contains inherent information on the strength of residential heating (L250). Wind direction indicates whether clean air from the west or more polluted air from the northeast is influencing the PM1 measurement. These mechanisms are mentioned in the introduction (L42-59) and the result section (chapter 4.2)
To convey these points more clearly to the reader, the following changes were made:

- *L85: added "atmospheric", changed "determining" to "influencing"*
- *L60: Added "...while moisture in the atmosphere can stimulate secondary particle formation processes…"*
- *L136-141: added in method section (chapter 2.2): "Following the objective of this study, a set of meteorological variables is chosen as inputs for the ML model that either influence PM concentrations directly via dilution (MLH, wind speed (ws), and wet scavenging of particles (precipitation)) and particle transport (wind direction as u, v components, air pressure (AirPres)), as a proxy for emissions (e.g. from residential heating: temperature at a height of 2 m (T)), and as a proxy for transformation processes (total incoming solar radiation (TISR), relative humidity (RH), T).*

The paper seems mostly focused on exploring the "SHapley Additive exPlanation(SHAP) values" approach and it is unclear whether a novel contribution has been made to the field of air pollution research. This paper may be better suited to a machine learn-ing journal or could be re-write to be more focused on air pollution. Either of these two options would require large changes to the current manuscript.
The novelty and also the advantage of the machine-learning framework is that all meteorological influences on PM1 concentrations are quantified at the same time, and interactions between the meteorological variables are captured. On this basis, their influence on any individual event can be separated and quantified (as done in

chapter 4.4). These aspects are novel and taken together, exceed the potential of past observation-based analyses.
It was not the aim of this study to explore the applicability SHAP values and it is unfortunate if this impression is conveyed by the current state of the manuscript. Therefore, extensive changes to the manuscript have been made to sharpen the scientific contribution of this manuscript and to more carefully emphasize scientific contributions.
Still, it is important to note here that much of the methodology chapter is dedicated to the ML algorithm and the SHAP values to make sure that the results chapter can be followed by readers not familiar with these techniques. An evaluation of the model such as in chapter 4.1 is critical to ensure that the model is able to reproduce empirical patterns.

Large parts of the abstract, introduction and the conclusion section were altered to shift the focus from the SHAP approach to the scientific findings. The following specific changes were made in the manuscript:

- *L510: removed "To our knowledge, this is the first time that the SHAP-framework for explainable machine learning is applied in atmospheric sciences"*
- *Headline 3.2: added "to infer processes" to stress the purpose of the SHAP values*
- *L211: was changed to "The interactions of input features contribute to the model output and thus reflect empirical patterns that are important to deepen the process understanding."*
- *L215: deleted from the manuscript "SHAP values are a novel tool to better understand multivariate natural systems, in particular when applied in state-of-the-art machine learning models as GBRT. So far, SHAP values have been used in the fields of computer science (Antwarg et al. 2019) and medical science (Lundberg et al., 2018b; Li et al., 2019a; Lundberg et al.,2020), but have yet to be applied to study environmental systems."*
- *L96: Removed "With the use of SHAP values, a detailed insight to the decisions of the statistical model can be provided, hence allowing an advancement of previous ML approaches (Friedman, 2001; Lundberg et al., 2018a)."*
- *L508-511: Removed "The GBRT approach in combination with the SHAP regression values presented here provides an intuitive tool to assess meteorological drivers of air pollution and to advance the understanding of high pollution events by uncovering different physical mechanisms leading to high-pollution episodes."*

- *L248: added "...as suggested by Fig. 5d..." to state more clearly that this constitutes a new finding*
- *L404-405: added "The physical explanation behind this pattern would be that lacking wet deposition and low wind speeds increase particle numbers in the atmosphere, while northeastern winds advect further particles. Given that there is now a large number of particles available, the accumulation effect of a low MLH is more efficient"*
- *See also changes in L96-103, which now more clearly pinpoint the purpose of the study*

Specific comments

Why has PM1 been the focus of this study, rather than the more health-relevant PM2.5species? Also, how did the model perform at predicting PM10? Considering the omis-sion of chemistry and emissions in this study, would PM10 or PM2.5 be a better candi-date for study?

The available ACSM instrumentation does process only PM1 particles. PM1 is highly relevant for human health, affecting the respiratory system. Smaller particles can penetrate deeper into the lungs compared to larger particles and potentially cause more damage Studies show that health impacts of PM1 are similar (Yang et al., 2018, DOI: 10.1016/S2542-5196(17)30100-6) or worse than PM2.5 (Chen et al. 2017, DOI: 10.1016/j.envint.2018.08.027). In addition, a study by the WHO indicates that BC is a good indicator for human health, which is most prominent for particles smaller 1µm (see https://www.euro.who.int/en/health-topics/environment-and-health/air-quality/publications/2012/health-effects-of-black-carbon-2012)

- *A comparison to PM10/PM2.5 is currently not feasible since no simultaneous measurements of PM1, PM2.5, PM10 and meteorological parameters at the same site are available*
- *Added to L111: "..., a highly health relevant fraction of PM including small particles that can penetrate deep into the lungs (Yang et al., 2018; Chen et al., 2017a)"*

Line 21 - "Processes vary even within seasons"This does not read well. Of course, processes will vary within seasons.

Sentence was removed from the manuscript.

Line 24 - “likely causes an increase in local wood-burning emissions”Cause and effect seem to be muddled. Maybe the authors mean to say increases in burning emission could explain increased particulates?

Yes, this was the intention. To make this more clear, the sentence was changed to “likely triggers increased local wood-burning emissions, which increase PM1 concentrations”

line 25 - “The application of SHAP regression values within a machine learning frame-work presents a novel and promising way of analysing observational data sets in envi-ronmental sciences.”Are there implications for what we should focus on meteorology studies or observations on? What about the implications for air-quality modelling or policy? Just presenting another tool that can be used is not a notable contribution.

This sentence was removed from the manuscript and replaced by “The identification of these meteorological conditions that increase air pollution could help policy makers to issue warnings to the public or install preemptive measures by specifically accounting for meteorological variability that influences PM1 concentrations. Furthermore, the presented framework has the potential to assess the effectiveness of air pollution measures.” L8 was changed to …”Based on the model, an isolation and quantification of individual meteorological influences for process understanding is achieved...”

See also changes in the introduction (L98-106) and conclusion (L502-510).

Line 90 - How can policymakers use this information? Improve air quality models?Focus research directions? What about it is new?

Extensive changes in the manuscript have been made in L96-103 (see also previous answers). In addition, potential applications and the new insights were emphasized in various parts of the conclusion section (L475-480, L502-510, L515-520).

L482-485: changed to “For policy makers, the presented approach could prove beneficial in multiple ways and serve as a decision aid for air policy measures. Another application would be to attribute changes in air quality to policy measures by comparing an ‘expected’ level of air pollution under given meteorological conditions to actual observations (e.g.,Cermak2009 and Knutti 2009), which may help…”

Line 90 - Why not focus on the SIRTA region, rather than Paris, which is in completely different chemistry and emissions regime? The reader needs to be convinced that the site is representative of the Paris region.
The results relate to the measurement site, which is representative of the Paris region background values. This was added in L127: "PM1 measurements are representative of background pollution levels of the region of Paris (Petit2015 et al., 2015)"
Sentence was rephrased in L94 "govern pollution concentrations at the measurement site" instead of "lead to high pollution events in Paris"

Technical comments

Please use sub/superscripts for chemical species throughout (e.g. SO42-, SO2,PM2.5).
This was adjusted accordingly.

Expand acronyms in sub-header titles (e.g. MLH).
This was adjusted accordingly.

Expand acronyms once per major section too.
Given the limited number of acronyms, the authors propose to extend them only at the first mention.

Meteorology-driven variability of air pollution (PM_1) revealed with explainable machine learning

Roland Stirnberg[1,2], Jan Cermak[1,2], Simone Kotthaus[3], Martial Haeffelin[3], Hendrik Andersen[1,2], Julia Fuchs[1,2], Miae Kim[1,2], Jean-Eudes Petit[4], and Olivier Favez[5]

[1]Institute of Meteorology and Climate Research, Karlsruhe Institute of Technology (KIT), Karlsruhe, Germany
[2]Institute of Photogrammetry and Remote Sensing, Karlsruhe Institute of Technology (KIT), Karlsruhe, Germany
[3]Institut Pierre Simon Laplace, École Polytechnique, CNRS, Institut Polytechnique de Paris, Palaiseau, France
[4]Laboratoire des Sciences du Climat et de l'Environnement, CEA/Orme des Merisiers, Gif sur Yvette, France
[5]Institut National de l'Environnement Industriel et des Risques, Parc Technologique ALATA, Verneuil en Halatte, France

Correspondence: Roland Stirnberg (Roland.Stirnberg@kit.edu)

Abstract. Air pollution, in particular high concentrations of particulate matter smaller than 1 μm in diameter (PM_1), continues to be a major health problem, and meteorology is known to RS: ~~substantially contribute to~~substantially influence atmospheric PM concentrations. However, the scientific understanding of the HA: ways by which complex HA: ~~mechanisms~~interactions of meteorological factors lead to high pollution episodes is inconclusive, as the effects of meteorological variables are not easy to separate and quantify. In this study, a novel, data-driven approach based on empirical relationships is used to characterise HA: ~~the role of meteorology on atmospheric concentrations of PM_1~~, and better understand the meteorology-driven component of PM_1 variability. A tree-based machine learning model is set up to reproduce concentrations of speciated PM_1 at a suburban site southwest of Paris, France, using meteorological variables as input features. RS: Based on the model, an isolation and quantification of individual meteorological influences for process understanding is achieved RS: ~~the contributions of each meteorological feature to modeled PM1 concentrations is quantified~~ using SHapley Additive exPlanation (SHAP) regression values. RS: ~~Meteorological contributions to PM_1 concentrations~~ RS: Season-specific processes influencing PM1 concentrations at the measurement site are analysed in selected high-resolution case studies.RS: ~~, contrasting season-specific processes.~~ Model results suggest that winter pollution episodes are often driven by a combination of shallow mixed layer heights (MLH), low temperatures, low wind speeds or inflow from northeastern wind directions. Contributions of MLHs to the winter pollution episodes are quantified to be on average ~5 μg/m^3 for MLHs below <500 m agl. Temperatures below freezing initiate formation processes and increase local emissions related to residential heating, amounting to a contribution RS: to predicted PM_1 concentrations of as much as ~9 μg/m^3. Northeasterly winds are found to contribute ~5 μg/m^3 to RS: ~~total~~predicted PM_1 concentrations (combined effects of u- and v-wind components), by advecting particles from source regions, e.g. central Europe or the Paris region. However, in calm conditions (i.e. wind speeds < ~2 m/s), the lack of dispersion leads to increased PM_1 concentrations by ~3 μg/m^3. Unusually high PM_1 concentrations in summer are generally lower compared to winter peak concentrations, and are characterised by a higher content of organics. Meteorological drivers of summer peak PM_1 concentrations are temperatures above ~25 °C (contributions of up to ~2.5 μg/m^3), dry spells of several days (maximum contributions of ~1.5 μg/m^3) and wind speeds below ~2 m/s (maximum contributions of ~3 μg/m^3). High-resolution case studies show a large variability of processes, which together lead to high PM_1 concentrations. RS: ~~Processes~~

~~vary even within seasons.~~ A high pollution episode in January 2016 is shown to be driven by a drop in temperature (maximum contributions of 11 μg/m^3), which enhances formation of secondary inorganic aerosols (SIA) and *RS:* ~~likely causes an increase in local wood-burning emissions~~likely triggers increased local wood-burning emissions, which increase PM_1 concentrations. In contrast, during December 2016, high PM_1 concentrations are caused mainly by a shallow MLH and low wind speeds. It is shown that an observed decrease in pollution levels is linked to a change in wind direction, advecting cleaner, maritime air to the PM measurement site (combined contributions of u- and v-wind-components of $\sim$-4 μg/m^3). *RS:* ~~The application of SHAP regression values within a machine learning framework presents a novel and promising way of analysing observational data sets in environmental sciences.~~ *RS:* The identification of these meteorological conditions that increase air pollution could help policy makers to issue warnings to the public or install preemptive measures by specifically accounting for meteorological variability that influences PM1 concentrations. Furthermore, the presented approach has the potential to realistically assess the effectiveness of air pollution measures.

1 Introduction

Air pollution has serious implications on human well-being, including deleterious effects on the cardiovascular system and the lungs (Hennig et al., 2018; Lelieveld et al., 2019), and an increased number of asthma seizures (Hughes et al., 2018). This includes particles smaller than 1 μm in diameter (PM_1), which are associated with fits of coughing (Yang et al., 2018) and an increase in emergency hospital visits (Chen et al., 2017b). The adverse health effect lead to an increase in mortality of people exposed to high particle concentrations (Samoli et al., 2008, 2013; Lelieveld et al., 2015). People living in urban areas are particularly affected by poor air quality and with increasing urbanization, their number is projected to grow (Baklanov et al., 2016; Li et al., 2019). These developments have motivated several countermeasures to improve air quality. Proposed efforts to reduce anthropogenic particle emissions include partial traffic bans (Su et al., 2015; Dey et al., 2018) and the reduction of solid fuel use for domestic heating (Chafe et al., 2014). Although emissions play an important role for PM concentrations in the atmosphere, meteorological conditions related to large-scale circulation patterns as well as local-scale boundary layer processes and interactions with the land surface are major drivers of PM variability as well (Cermak and Knutti, 2009; Bressi et al., 2013; Megaritis et al., 2014; Dupont et al., 2016; Petäjä et al., 2016; Yang et al., 2016; Li et al., 2017). *RS:* ~~It is therefore crucial to take atmospheric and environmental processes into account during the development of efficient pollution mitigation strategies~~. Wind speed and direction generally have a strong influence on air quality as they determine the advection of pollutants (Petetin et al., 2014; Petit et al., 2015; Srivastava et al., 2018). Limiting the vertical exchange of air masses, the mixed layer height (MLH) governs the volume of air in which particles are typically dispersed. Although some authors indicate that mixed layer height cannot be related directly to concentrations of pollutants and that other meteorological parameters and local sources need to be considered (Geiß et al., 2017), a lower MLH can increase PM concentrations as particles are not mixed into higher atmospheric levels and accumulate near the ground (Gupta and Christopher, 2009; Schäfer et al., 2012; Stirnberg et al., 2020).

Higher MLHs in combination with high wind speeds increase atmospheric ventilation processes, thus decreasing near-surface particle concentrations (Sujatha et al., 2016; Wang et al., 2018). Air temperature can influence PM concentrations in multiple ways, e.g. by modifying the emission of secondary PM precursors such as volatile organic compounds (VOCs) during summer (Fowler et al., 2009; Megaritis et al., 2013; Churkina et al., 2017), and by condensating high saturation vapour pressure compounds such as nitric acid and sulfuric acid (Hueglin et al., 2005; Pay et al., 2012; Bressi et al., 2013; Megaritis et al., 2014). The wet removal of particles by precipitation is known to be an efficient atmospheric aerosol sink (Radke et al., 1980; Bressi et al., 2013), RS: while moisture in the atmosphere can stimulate secondary particle formation processes (Ervens et al., 2011). Although all these atmospheric conditions and processes have been identified as drivers of local air quality, it is usually a complex combination of meteorological and chemical processes that lead to the formation of high-pollution events (Petit et al., 2015; Dupont et al., 2016; Stirnberg et al., 2020).

The metropolitan area of Paris is one of the most densely populated and industrialised areas in Europe. Thus, air quality is a recurring issue and has been at the focus of many studies in the past years (Bressi et al., 2014; Petetin et al., 2014; Petit et al., 2015; Dupont et al., 2016; Petit et al., 2017; Srivastava et al., 2018). Results indicate that the Paris metropolitan region is often affected by mid- to long-range transport of pollutants, as due to the city's flat orography, an efficient horizontal exchange of air masses is frequent (Bressi et al., 2013; Petit et al., 2015). High-pollution events commonly occur in late autumn, winter, and early spring. Often, these episodes are characterised by stagnant atmospheric conditions and a combination of local contributions, e.g. traffic emissions, residential emissions, or regionally transported particles, e.g. ammonium nitrates from manure spreading, or sulfates from point sources (Petetin et al., 2014; Petit et al., 2014, 2015; Srivastava et al., 2018). High-pressure conditions with air masses originating from continental Europe (Belgium, Netherlands, West Germany) are generally associated with an increase in particle concentrations, especially of secondary inorganic aerosols (SIA, Bressi et al. (2013); Srivastava et al. (2018). The regional contribution has been found to be in the range of 70 % for background concentrations in Paris of particles with a diameter smaller 2.5 μm (Petetin et al., 2014). Hence the variability between high-pollution episodes in terms of timing, sources and meteorological boundary conditions is considerable (Petit et al., 2017). Previous approaches to determine meteorological drivers of air pollution included, for example, the use of chemical transport models (CTMs), which, however, require comprehensive knowledge on emission sources and secondary particle formation pathways and are associated with considerable uncertainties (Sciare et al., 2010; Petetin et al., 2014; Kiesewetter et al., 2015). Further methods rely on data exploration, e.g. the statistical analysis of time-series (Dupont et al., 2016), which can be coupled with positive matrix factorization (PMF, Paatero and Tapper, 1994) to derive PM sources (Petit et al., 2014; Srivastava et al., 2018). To take into account the interconnected nature of PM drivers, multivariate statistical approaches such as principal component analysis (PCA) have been applied (Chen et al., 2014; Leung et al., 2017). In recent years, machine learning techniques have been increasingly used to expand the analysis of PM concentrations with respect to meteorology, allowing to retrace general patterns (Hu et al., 2017; Grange et al., 2018).

Here, the multivariate and highly interconnected RS: nature of meteorology-dependent atmospheric processes influencing RS: ~~nature of the processes determining~~ local PM_1 concentrations RS: at a suburban site southwest of Paris is RS: ~~captured and~~ analysed in a data-driven way. RS: Therefore, a state-of-the-art explainable machine learning model is set up to reproduce the variability of

PM_1 concentrations, thereby capturing empirical relationships between PM_1 concentrations and meteorological parameters. RS: ~~A state-of-the-art explainable machine learning model is set up to reproduce the variability of PM_1 concentrations~~, RS: The goal is to separate and quantify influences of the meteorological variables on PM_1 concentrations to advance RS: ~~with the objective of advancing~~ the process understanding of the complex mechanisms that RS: ~~lead to high pollution events in Paris~~govern pollution concentrations at the measurement site. Localised (i.e. situation-based) and individualised attributions of feature contributions are performed using SHapley Additive exPlanation regression (SHAP) values (Lundberg and Lee, 2017; Lundberg et al., 2018a, 2020), RS: allowing to infer meteorology-dependent processes driving PM concentrations at high temporal resolution. RS: ~~With the use of SHAP values, a detailed insight to the decisions of the statistical model can be provided, hence allowing an advancement of previous ML approaches~~ RS: ~~The attribution of local (i.e. situation-based) statistical feature contributions enables quantitative estimates of meteorological drivers of PM concentrations and allows to infer meteorology-dependent processes driving PM concentrations at high temporal resolution.~~ RS: Typical situations that lead to high PM_1 concentrations are identified, serving as a decision support to policymakers to issue preventative warnings to the public if these situations are to be expected. In addition, by directly accounting for meteorological effects on PM1 concentrations, such a machine learning-based framework could help in assessing the effectiveness of measures towards better air quality. ~~Meteorological effects on speciated PM_1 concentrations are quantified and the roles of the most critical atmospheric variables for driving peak particle concentrations are highlighted. The improved scientific understanding of processes is crucial for the assessment of the effectiveness of measures towards better air quality, and therefore of high value to political decision makers.~~ RS: Furthermore, the proposed ML framework can be viewed as a first step towards a data-driven, prognostic tool in operational air quality forecasting, complementary to CTM approaches.

2 Data sets

Seven years (2012-2018) of meteorological and air quality data from the Site Instrumental de Recherche par Télédétection Atmosphérique (SIRTA, Haeffelin et al., 2005) supersite are the basis of this study. The SIRTA Atmospheric Observatory is located about 25km southwest of Paris (48.713°N and 2.208°E, Fig. 1). This study focuses on day-to-day variations of total and speciated PM_1 RS:, a highly health relevant fraction of PM including small particles that can penetrate deep into the lungs (Yang et al., 2018; Chen et al., 2017a). To separate diurnal effects e.g. the development of the boundary layer during morning hours (Petit et al., 2014; Dupont et al., 2016; Kotthaus and Grimmond, 2018a) from day-to-day variations of PM_1, mean concentrations of total and speciated PM_1 for the afternoon period 12-15 UTC are considered, when the boundary layer is fully developed. In sections 2.1 and 2.2, the PM_1 and meteorological data and preprocessing steps before setting up the machine learning model are described. The applied machine learning model and data analysis techniques are presented in sections 3.1 and 3.2.

2.1 Submicron particle measurements

Aerosol chemical speciation monitor (ACSM, Ng et al., 2011) measurements are conducted at SIRTA in the framework of the ACTRIS project. The ACSM provides continuous and near real-time measurements of the major chemical composition of non-refractory submicron aerosols, i.e., organics (Org), ammonium (NH_4^+), sulfate (SO_4^{2-}), nitrate (NO_3^-) and chloride (Cl^-).

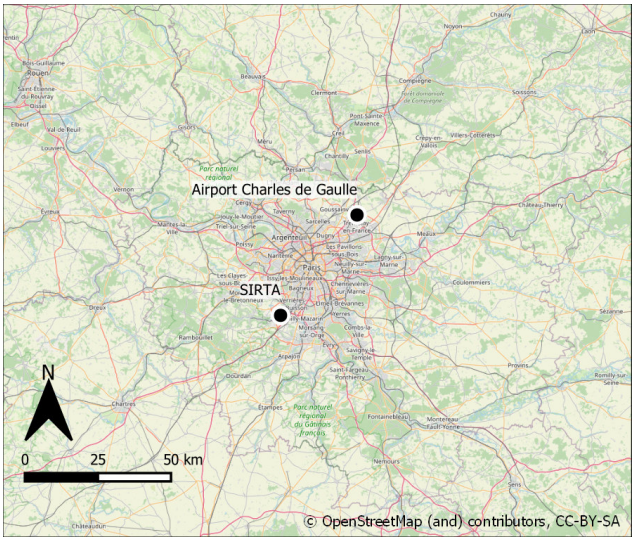

Figure 1. Location of the SIRTA supersite southwest of Paris. © OpenStreetMap contributors 2020. Distributed under a Creative Commons BY-SA License.

A detailed description of its functionality can be found in Ng et al. (2011). Data processing and validation protocol can be found in Petit et al. (2015) and Zhang et al. (2019). In addition, black carbon (BC) has been monitored by a seven-wavelength Magee Scientific Aethalometer AE31 from 2011 to mid-2013, and a dual-spot AE33 (Drinovec et al., 2015) from mid-2013 onwards. Consistency of both instruments have been checked in Petit et al. (2014). Using the multispectral information, a differentiation into fossil fuel-based BC (BCff) and BC from wood burning (BCwb) is achieved (Sciare et al., 2010; Healy et al., 2012; Petit et al., 2014; Zhang et al., 2019). Here, the sum of all measured species is assumed to represent the total PM_1 content (see Petit et al., 2014, 2015). The consistency of ACSM and Aethalometer measurements is checked by comparing the sum of all monitored species with measurements of a nearby Tapered Element Oscillating Microbalance equipped with a Filter Dynamic Measurement System (TEOM-FDMS). *RS:* PM_1 measurements are representative of suburban background pollution levels of the region of Paris (Petit et al., 2015). As an additional input to the machine learning model, the average fraction of NO_3^- of the previous day is added (NO3_frac). Pollution events dominated by NO_3^- are often linked to regional-scale events, which depend on anthropogenically-influenced processes in the source regions of NO_3^- precursors (Petit et al., 2017). This is approximated by the inclusion of the average fraction of NO_3^- of the previous day, assuming that a high fraction of NO_3^- indicates the occurrence of such an anthropogenically-influenced regime.

2.2 Meteorological data

RS: ~~Meteorological variables included in this study are ambient air temperature (at a height of 2 m, T), relative humidity (RH), ambient air pressure (AirPres), precipitation, wind speed (ws), wind direction (u, v components) and total incoming solar radiation (TISR).~~ Following the objective of this study, a set of meteorological variables is chosen as inputs for the ML model that either influence PM concentrations directly via

dilution (MLH, wind speed (ws), and wet scavenging of particles (precipitation)) and particle transport (wind direction as u, v components, air pressure (AirPres)), as a proxy for emissions (e.g. from residential heating: temperature at a height of 2 m (T)), and as a proxy for transformation processes (total incoming solar radiation (TISR), relative humidity (RH), T). Data are taken from the quality-controlled and 1h averaged re-analysed observation (ReObs) dataset. Further information on the instrumentation used for the acquisition of these variables is provided in Chiriaco et al. (2018). MLH is derived from automatic lidar and ceilometer (ALC) measurements of a Vaisala CL31 ceilometer using the CABAM algorithm (Characterising the Atmospheric Boundary layer based on ALC Measurements, Kotthaus and Grimmond, 2018a, b). Due to an instrument failure, during the period July to mid-November 2016, SIRTA ALC measurements had to be replaced with measurements conducted at the Paris Charles de Gaulle Airport, located northeast of Paris. *RS:* A comparison of measured MLHs at SIRTA and Charles de Gaulle Airport for the available measurements in 2016 (Appendix A) shows generally good agreement, which is why only minor uncertainties are expected due to the replacement.

Meteorological factors are chosen as input features for the statistical model based on findings of previous studies (see section 1). Meteorological observations are converted to suitable input information for the statistical model (see section 3.1). Wind speed (ws) is derived from the ReObs u and v components [m/s] and the maximum wind speed of the afternoon period (12-15 UTC) is included in the model. U and v wind components are then normalised to values between 0 and 1, thus only depicting the direction information. To reduce the impact of short-term fluctuation in wind direction, the 3-day running mean is calculated based on the normalised u and v wind components (umean and vmean). Hours since the last precipitation event (Tprec) are counted and used as input to capture the particle accumulation effect between precipitation events (Rost et al., 2009; Petit et al., 2017).

3 Methods

3.1 Machine learning model: technique and application

Gradient Boosted Regression Trees (GBRT, used here in a python 3.6.4 environment with the scikit-learn module, Friedman, 2002; Pedregosa et al., 2012) are applied to predict daily total and speciated PM_1 concentrations. As a tree-based method, GBRTs use a tree regressor, which sets up decision trees based on a training data set. The trees split the training data along decision nodes, creating homogeneous subsamples of the data by minimizing the variance of each subsample. For each subsample, regression trees fit the mean response of the model to the observations (Elith et al., 2008). To increase confidence in the model outputs, decision trees are combined to form an ensemble prediction. Trees are sequentially added to the ensemble (Elith et al., 2008; Rybarczyk and Zalakeviciute, 2018) and each new tree is fitted to the predecessor's previous residual error using gradient descent (Friedman, 2002). This is an advantage of GBRT over standard ensemble tree methods (e.g. Random Forests (RF), Just et al., 2018) as trees are built systematically and fewer iterations are required (Elith et al., 2008). Characteristics of the meteorological training data set with respect to observed total and speciated PM_1 concentrations are conveyed to the statistical model. The learned relationships are then used for model interpretation and to produce estimates of PM_1 based on unseen meteorological data to test the model. The architecture of the statistical model is determined by the hyperparameters,

e.g. the number of trees, the maximum depth of each tree (i.e., the number of split nodes on each tree) and the learning rate (i.e., the magnitude of the contribution of each tree to the model outcome, which is basically the step size of the gradient descent). The hyperparameters are tuned by executing a grid search, systematically validating testing previously defined hyperparameter combinations and determining the best combination via a three-fold cross validation. Note that PM_1 data is not normally distributed, i.e. there is more data available for mid-range concentrations. To avoid that the model primarily optimizes its predictions on these values, a least-squares loss function was chosen. This loss function is more sensitive to higher PM_1 values (i.e. outliers of the PM_1 data distribution), as it strongly penalises high absolute differences between predictions and observations. Accordingly, the model is adjusted to reproduce higher concentrations as well.

For each PM species, a specific GBRT model is set up and used for the analysis of meteorological influences on individual PM_1 species (see section 4.2). Additionally, a quasi-total PM_1 model is used to reproduce the sum of all species at once, which is used for an analysis of meteorological drivers of high-pollution events (see sections 4.3 and 4.4). Train and test data sets to evaluate each model are created by randomly splitting the full data set. These splits, however, are the same for the species models and the full PM_1 model to ensure comparability between the models. Three quarters of the data are used for training and hyperparameter tuning with cross-validation (n=1086), and one quarter for testing (n=363). In addition, the robustness of the model results is tested by repeating this process ten times, resulting in ten models with different train-/ test-splits and different hyperparameters.

3.2 Explaining model decisions RS: to infer processes: SHapley Additive exPlanation (SHAP) values

While being powerful predictive models, tree-based machine learning methods also have a high interpretability (Lundberg et al., 2020). In order to understand physical mechanisms on the basis of model decisions, the contributions of the meteorological input features to the model outcome are analysed. Feature contributions are attributed using SHAP values, which allow for an individualised, unique feature attribution for every prediction (Shapley, 1953; Lundberg and Lee, 2017; Lundberg et al., 2018a, 2020). SHAP values provide a deeper understanding of model decisions than the relatively widely used partial dependence plots (Friedman, 2001; Goldstein et al., 2015; Fuchs et al., 2018; Lundberg et al., 2018a; McGovern et al., 2019; Stirnberg et al., 2020). Partial dependence plots show the global mean effect of an input feature to the model outcome, while SHAP values quantify the feature contribution to each single model output, accounting for multicollinearity. Feature contributions are calculated from the difference in model outputs with that feature present, versus outputs for a retrained model, without the feature. Since the effect of withholding a feature depends on other features in the model due to interactive effects between the features, differences are computed for all possible feature subset combinations of each data instance (Lundberg and Lee, 2017). Summing up SHAP values for each input feature at a single time step yields the final model prediction. SHAP values can be negative since SHAP values are added to the base value, which is the mean prediction when taking into account all possible input feature combinations. Negative (positive) SHAP values reduce (raise) the prediction below (above) the base value. The higher the absolute SHAP value of a feature, the more distinct is the influence of that feature on the model predictions. The sum of all SHAP values at one time step yields the final prediction of PM_1 concentrations. An example of breaking down a model prediction into feature contributions using SHAP values is shown schematically in Fig. 2. The computation of traditional

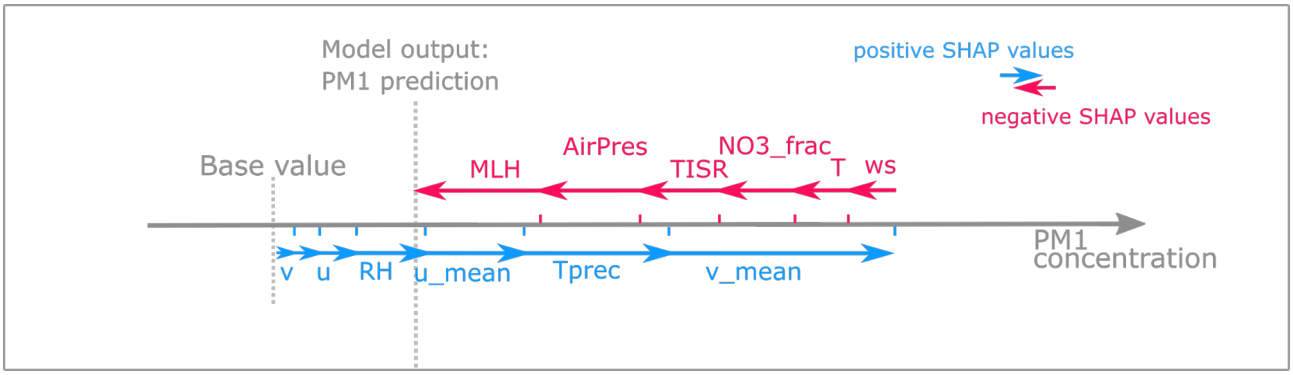

Figure 2. Conceptual figure illustrating the interaction of SHAP values and model output. Starting with a base value, which is the mean prediction if all data points are considered, positive SHAP values (blue) increase the final prediction of total and speciated PM_1 concentrations, while negative SHAP values (red) decrease the prediction. The sum of all SHAP values for each input feature yields the final prediction. Depending on whether positive or negative SHAP values dominate, the prediction is higher or lower than the base value (Lundberg et al., 2018b). Adapted from https://github.com/slundberg/shap.

Shapley Regression values is time consuming, since a large number of all possible feature combinations have to be included. The SHAP framework for tree-based models allows a faster computation compared to full shapley regression values while maintaining a high accuracy (Lundberg and Lee, 2017; Lundberg et al., 2018a) and is therefore used here. The shap python implementation is used for the computation of SHAP values (https://github.com/slundberg/shap).

RS: ~~Pairwise interactive effects between input features can be estimated using the SHAP approach.~~ The interactions of input features contribute to the model output and thus reflect empirical patterns that are important to deepen the process understanding. Interactive effects are defined as the difference between the SHAP values for one feature when a second feature is present and the SHAP values for the one feature when the other feature is absent (Lundberg et al., 2018a). *RS:* ~~SHAP values are a novel tool to better understand multivariate natural systems, in particular when applied in state-of-the-art machine learning models as GBRT. So far, SHAP values have been used in the fields of computer science and medical science , but have yet to be applied to study environmental systems.~~

4 Results and discussion

4.1 Model performance

The performance of the ten model iterations is assessed by comparing the coefficient of determination (R^2) and normalised root mean square error (NRSME) for the independent test data that was withheld during the training process (Fig. 3). While the models for BCwb, BCff and total PM_1 show small spread, Cl^- and NO_3^- exhibit larger variations between model runs (indicated by horizontal and vertical lines in Fig. 3). This suggests that while drivers of variations in BCff concentration are well covered by the model, this is less so in the case of Cl^- and NO_3^-. Possible reasons for this are that no explicit information on anthropogenic emissions or chemical formation pathways are included in the models. Still, the model performance indicators

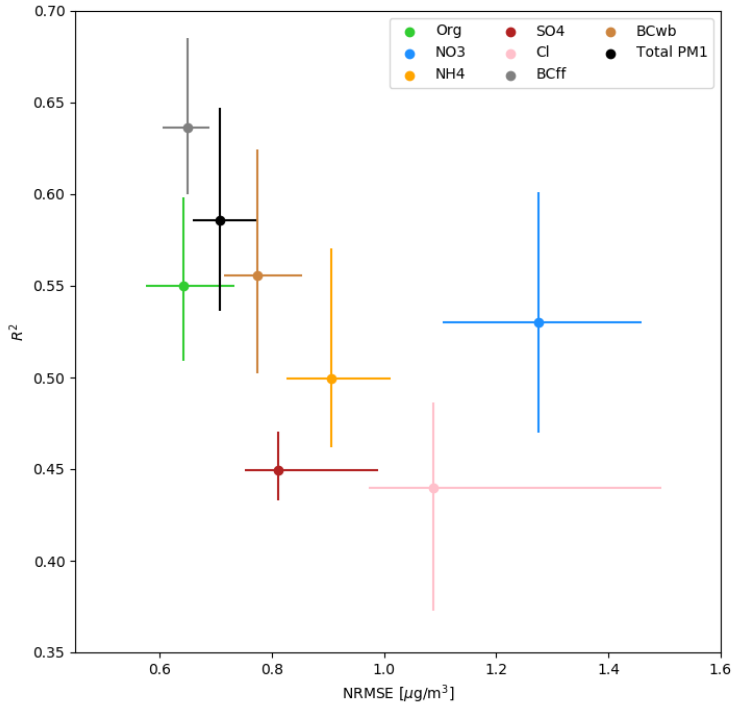

Figure 3. Performance indicators for ten model iterations: coefficient of determination R^2 against normalised Root Mean Squared Error (NRMSE) for the separate species models and the total PM_1 model. Vertical and horizontal lines indicate the maximum spread in R^2 and NRMSE, respectively.

highlight that a large fraction of the variations in particle concentrations are explained by the meteorological variables used as model inputs. Performances of model iterations of the species-specific and total PM_1 are generally similar, suggesting a robust model outcome.

The mean input feature importance, ordered from high to low, of the total PM_1 model run by means of the SHAP feature attribution values is shown in Fig. 4, The NO_3^- fraction of the previous day has the highest impact on the model, followed by temperature, wind direction information, and MLH. To some extent, NO_3^- fraction can be related to PM_1 mass concentrations (Petit et al., 2015; Beekmann et al., 2015). This means that the higher the PM_1 levels one day, the greater the chances of having higher PM_1 levels the next day. The impact of the meteorological variables on model decisions is analysed in more detail in the following.

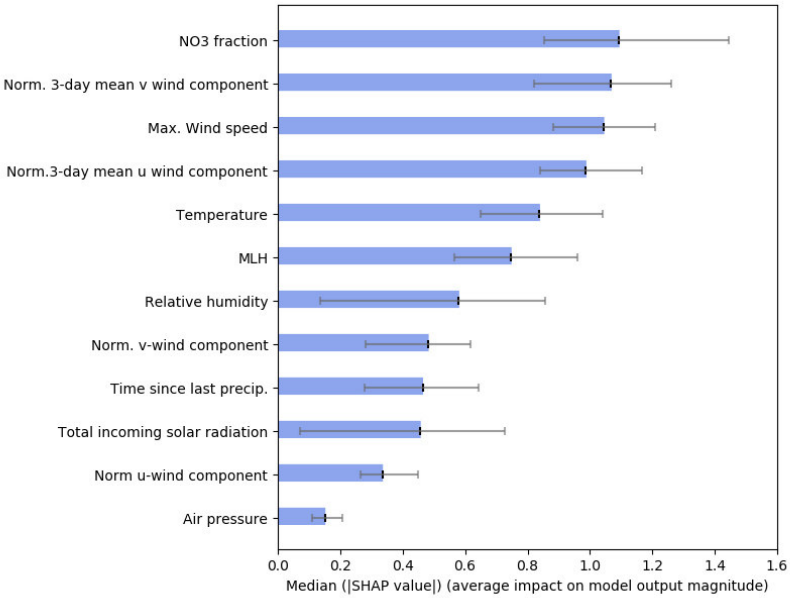

Figure 4. Ranked median SHAP values of the model input features, i.e. the average absolute value that a feature adds to the final model outcome, referring to the total PM_1 model [$\mu g/m^3$] (Lundberg et al., 2018b). Horizontal lines indicate the variability between model runs.

4.2 RS: ~~Contribution~~Influence of meteorological input features on modelled particle species and total PM_1 concentrations

To gain insights on relevant processes governing particle concentrations RS: ~~in the Paris region~~at SIRTA, the contribution of input features on species and total PM_1 concentration outcomes from the statistical model, i.e. the SHAP values, are plotted as a function of absolute feature values (Figs 5-7). The contribution of an input feature to each (local) prediction of the species or total PM_1 concentrations is shown while taking into account intra-model variability. Intra-model variability of SHAP values, i.e. different SHAP value attributions for the same feature value within one model, is shown by the vertical distribution of dots for absolute input feature values. Intra-model variability is caused by interactions of the different model input features.

4.2.1 RS: ~~Contribution~~Influence of temperature

The impact of ambient air temperature on modelled species concentrations is highly non-linear (Fig. 5). All species show increased contributions to model outcomes at temperatures below $\sim$4 °C while the contribution of high temperatures on model outcomes differs substantially between species. The statistical model is able to reproduce well-known characteristics of species concentration variations related to temperature. For example, sulfate formation is enhanced with increasing temperatures (Fig. 5d) due to an increased oxidation rate of SO_2 (see Dawson et al., 2007; Li et al., 2017) and strong solar irradiation due to

photochemical oxidation (Gen et al., 2019). Dawson et al. (2007) reported an increase of 34 ng/m^{3}K for $PM_{2.5}$ concentrations using a CTM. The increase in sulfate at low ambient temperatures RS: as suggested by Fig. 5d is not reported in this study. It is likely linked to increased aqueous phase particle formation in cold and foggy situations (Rengarajan et al., 2011; Petetin et al., 2014; Cheng et al., 2016). Considerable local formation of nitrate at low temperatures (Fig. 5b) is consistent with results from previous studies in western Europe and enhanced formation of ammonium nitrate at lower temperatures (Fig. 5c) by the shifting gas-particle equilibrium is a well-known pattern (e.g., Clegg et al., 1998; Pay et al., 2012; Bressi et al., 2013; Petetin et al., 2014; Petit et al., 2015). The increase in organic matter and BCwb concentrations at low temperatures (Fig. 5g) is likely related to the emission intensity, as biomass burning is often used for domestic heating in the study area (Favez et al., 2009; Sciare et al., 2010; Healy et al., 2012; Jiang et al., 2019). In addition, organic matter concentrations are linked to the condensation of semi-volatile organic species at low temperatures (Putaud et al., 2004; Bressi et al., 2013). The sharp increase in modelled concentrations of organics above 25°C (Fig 5a) could be due to enhanced biogenic activity leading to a rise in biogenic emissions and secondary aerosol formation (Guenther et al., 1993; Churkina et al., 2017; Jiang et al., 2019).

The contribution of temperature on modelled total PM_1 concentrations (Fig. 6h) is consistent with the response patterns to changes in temperatures described for the individual species in panels 6a-6g, with positive contributions at both low (<4 °C) and high air temperatures (>25 °C). For temperatures below freezing, the model allocates maximum contributions to modelled total PM_1 concentrations of up to 12 μg/m^3. The spread of SHAP values between model iterations is generally higher for low temperatures (vertical grey bars in Fig. 6), where SHAP values are of greater magnitude, but in all cases the signal contained in the feature contributions far exceeds the spread between model runs.

4.2.2 RS: ~~Contribution~~Influence of RS: the mixed layer height (MLH)

Variations in MLH can have substantial impact on near-surface particle concentrations, as the mixed layer is the atmospheric volume in which the particles are dispersed (see Klingner and Sähn, 2008; Dupont et al., 2016; Wagner and Schäfer, 2017). The effect of MLH variations on modelled particle concentrations is highly nonlinear RS: and varies in magnitude for all species (Fig. 6)RS: ~~, with the magnitude of the contribution varying by species~~. RS: ~~Possible reasons for this will be discussed in the following~~. Similar to the patterns observed for temperature SHAP values, the inter-model variation of predictions is highest for low MLHs where predicted particle concentrations have the highest variation. RS: For predicted total PM_1 concentrations, the maximum positive contribution of the MLH is as high as 5.5 μg/m^3 while negative contributions can amount to -2 μg/m^3. While the maximum influence of MLH is lower than the maximum influence determined for air temperature, the frequency of shallow MLH is far greater than that of the minimum temperatures that have the largest effect (Figs 5d & 6d). Contributions of MLH to predicted particle concentrations are highest for very shallow mixed layers due to the accumulation of particles close to the ground RS: ~~under shallow MLH conditions~~ (Dupont et al., 2016; Wagner and Schäfer, 2017). RS: In addition to causing particles to accumulate near the surface, low MLH can also provide effective pathways for local new particle formation. Secondary pollutants, such as ammonium nitrate, are increased at low MLHs when conditions favorable to their formation usually coincide with reduced vertical mixing (i.e., low temperatures, often in combination with high RH, Pay et al., 2012; Petetin et al., 2014; Dupont et al., 2016; Wang et al., 2016). RS: BC concentrations, on the other hand, are dominated by primary emissions, as is a substantial fraction of organic

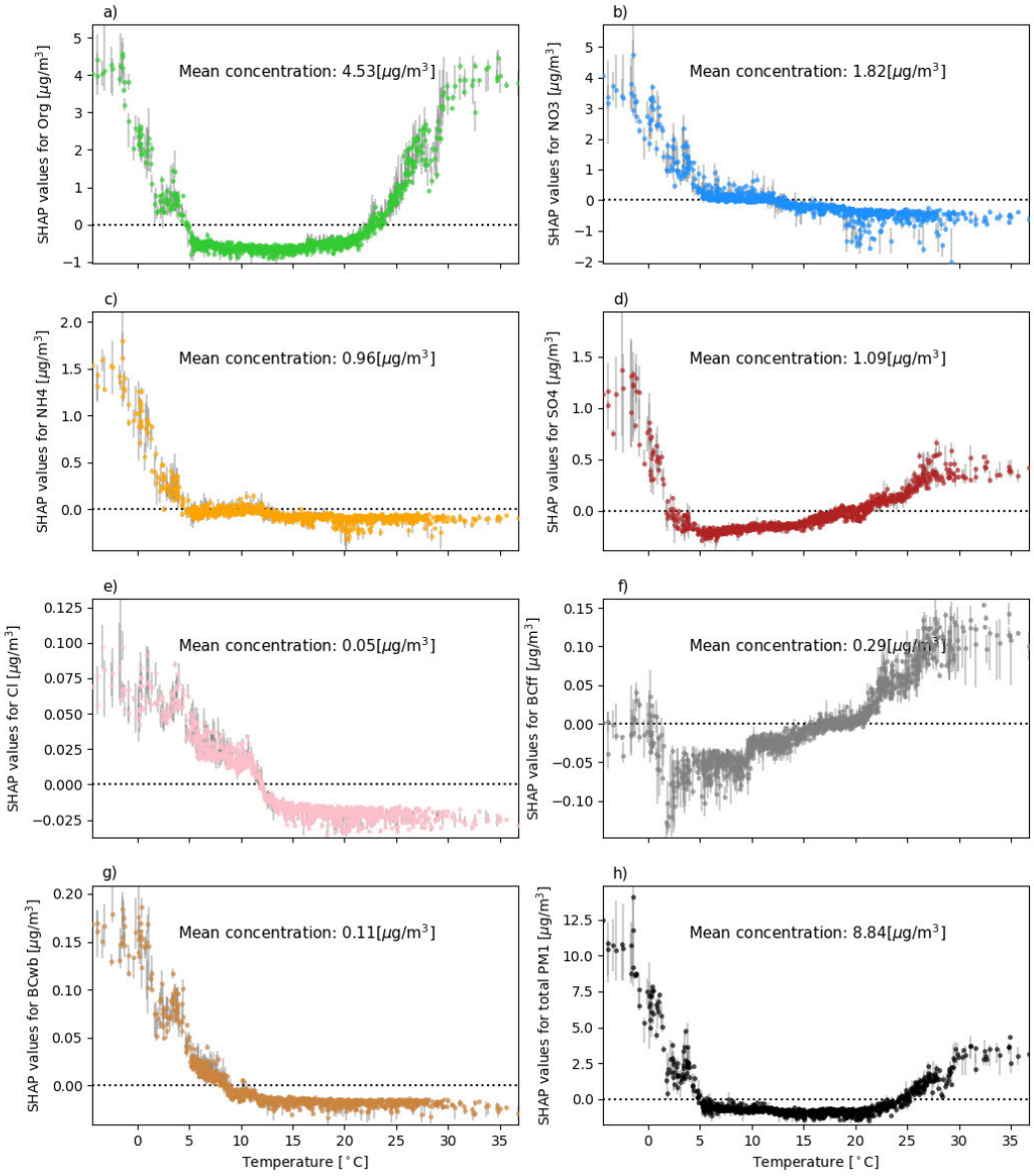

Figure 5. Air temperature SHAP values (contribution of temperature to the prediction of species and total PM_1 concentrations [$\mu g/m^3$] for each data instance) vs. absolute air temperature [°C]. Inter-model variability of allocated SHAP values is shown as the variance of predicted values between the ten model iterations and plotted as vertical grey bars. The dotted horizontal line indicates the transition from positive to negative SHAP values.

matter (Petit et al., 2015). *RS:* Hence, the accumulation of these particles during low buoyancy conditions can explain the strong influence of MLH on BCwb and BCff. A relatively distinct transition from positive contributions during shallow boundary

layer conditions (∼0–800 m) towards negative contributions at high MLHs is evident for all species except SO_4^{2-}. Modelled SO_4^{2-} concentrations show a less distinct response to changes in MLH as they are largely driven by gaseous precursor sources and particle advection, RS: both rather independent of MLH (Pay et al., 2012; Petit et al., 2014, 2015), so that the accumulation effect RS: ~~under low MLH conditions is hence~~ is less important. RS: ~~Furthermore, an~~The increase of SO_4^{2-} concentrations with higher MLHs (>∼ 1500 m agl) could RS: ~~be due to a more~~linked to the effective transport of SO_4^{2-} and its precursor SO_2 RS: ~~under high MLH conditions~~ (Pay et al., 2012).

In agreement with results from previous studies focusing on PM_{10} (Grange et al., 2018; Stirnberg et al., 2020) or $PM_{2.5}$ (Liu et al., 2018), SHAP values do not change much for MLH above ∼800–900 m, i.e. boundary layer height variations above this level do not influence submicron particle concentrations. Positive contributions of MLHs above ∼800–900 m RS: on predicted PM_1 concentrations, as visible in Fig. 6 RS: for some species, have been previously reported by Grange et al. (2018), who relate this pattern to enhanced secondary aerosol formation in a very deep and dry boundary layer. The positive RS: ~~contribution~~influence of high MLHs on species that are partly secondarily formed, e.g. SO_4^{2-} and Org, could be explained following this argumentation. However, processes driving the positive RS: ~~contribution~~influence of high MLHs on BCff, which is directly emitted to the atmosphere, remain inconclusive. RS: ~~For predicted total PM_1 concentrations, the maximum positive contribution of the MLH is as high as 5.5 $\mu g/m^3$ while negative contributions can amount to -2 $\mu g/m^3$. While the maximum influence of MLH is lower than the maximum influence determined for air temperature, the frequency of shallow MLH is far greater than that of the minimum temperatures that have the largest effect~~ RS: ~~In addition to causing particles to accumulate near the surface, low MLH can also provide effective pathways for local new particle formation. Secondary pollutants, such as ammonium nitrate, are increased at low MLHs when conditions favorable to their formation usually coincide with reduced vertical mixing~~ RS: ~~BC concentrations, on the other hand, are dominated by primary emissions, as is a substantial fraction of organic matter~~ RS: ~~Hence, the accumulation of these particles during low buoyancy conditions can explain the strong influence of MLH on BCwb and BCff.~~

4.2.3 RS: ~~Contribution~~Influence of wind direction

To analyse the contribution of wind direction to predicted particle concentrations, SHAP values of normalised 3-day mean u and v wind components were added up and transformed to RS: units of degrees (Fig. 7). Generally, wind direction has a positive contribution to the model outcome when winds from the northern to northeastern sectors prevail, while negative contributions are evident for southwesterly directions. Given the location of the measurement site, this pattern undoubtedly reflects the advection of particles emitted from continental Europe and/or RS: ~~Paris city centre~~the Paris metropolitan area under high pressure system conditions versus cleaner marine air masses during southwesterly flow (Bressi et al., 2013; Petetin et al., 2014; Petit et al., 2015; Srivastava et al., 2018). Increased concentrations of organic matter are predicted for northerly, northeasterly and easterly winds. These patterns suggest a significant contribution of advected organic particles from a specific wind sector. This is in agreement with the findings of Petetin et al. (2014) who estimated that 69 % of the PM25 organic matter fraction is advected by northeasterly winds, which is related to advected particles from wood burning sources in the Paris region and SOA formation along the transport trajectories. While Petit et al. (2015) did not find a wind direction dependence of organic matter measured at SIRTA using wind regression, they reported the regional background of organic matter to be of importance. Comparing upwind rural stations to urban sites, Bressi et al. (2013) concluded organic matter is largely driven by mid- to

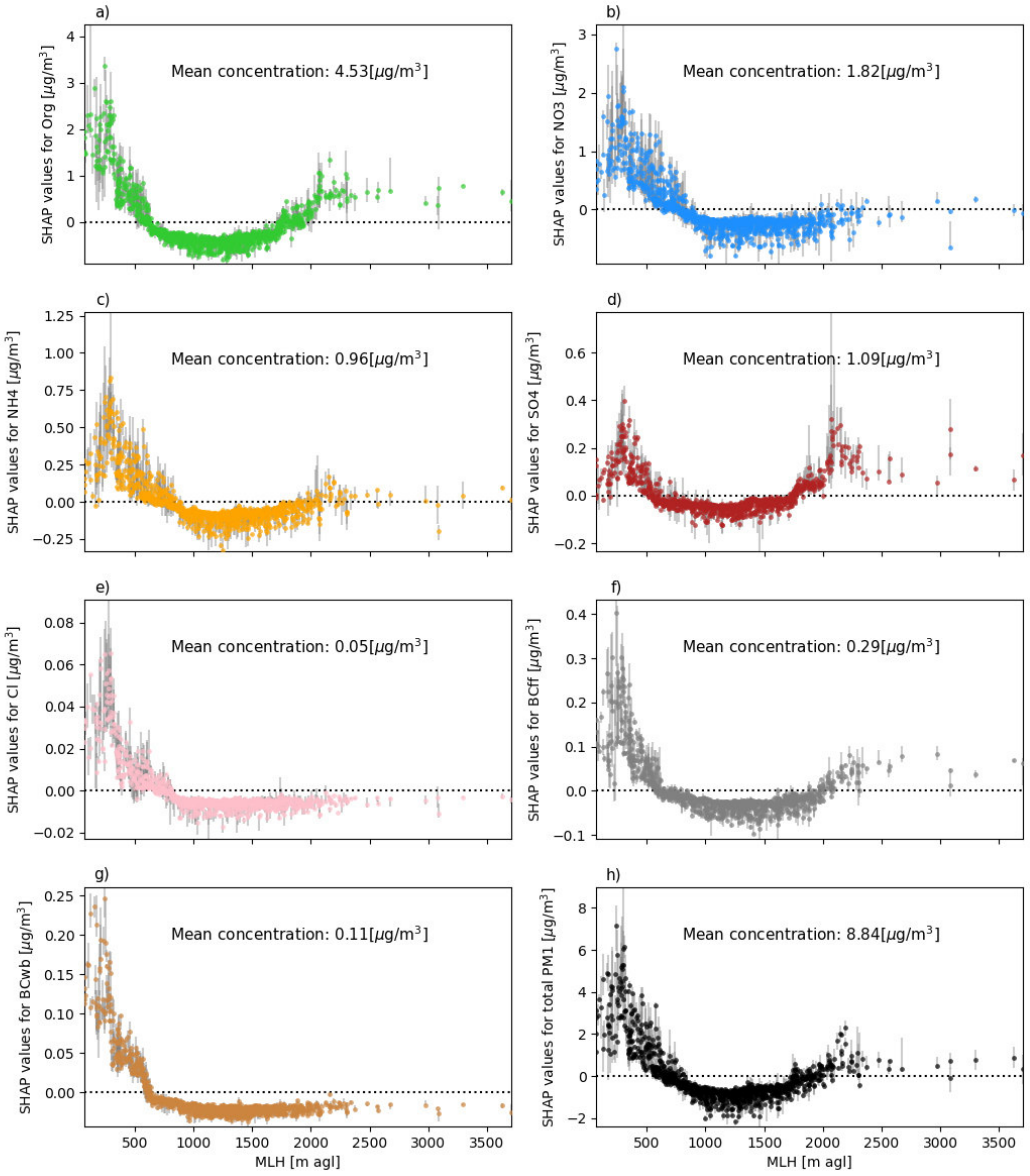

Figure 6. As Fig. 5 for MLH SHAP values (contribution of MLH to the prediction of species and total PM_1 for each data instance) vs. absolute MLH values [m agl].

long-range transport. RS: ~~Contributions to~~ Influences on the SO_4^{2-}-model are highest for northeastern and eastern wind direction, which aligns with previous findings by Pay et al. (2012); Bressi et al. (2014); Petit et al. (2017), who identified the Benelux region and western Germany as strong emitters of sulfur dioxide (SO_2). SO_2 can be transformed to particulate SO_4^{2-} (Pay et al., 2012) while being transported towards the measurement site. Nitrate concentrations are affected by long-range transport from

continental Europe (Benelux, western Germany), which are RS: ~~imported~~advected towards SIRTA from northeastern directions (Petetin et al., 2014; Petit et al., 2014). It is to be expected that the influence of mid- to long-range transport on the particle observations at SIRTA is rather substantial, with most high pollution days affected by particle advection from continental Europe (Bressi et al., 2013). Concerning BCff and BCwb, model results suggest a dependence on wind direction during northwestern to northeastern inflow. Although BC concentrations are expected to be largely determined by local emissions (Bressi et al., 2013), e.g. from local residential areas, a substantial contribution of imported particles from wood burning and traffic emissions from the Paris RS: ~~city centre~~region (Laborde et al., 2013; Petetin et al., 2014) and continental sources is likely (Petetin et al., 2014).

4.2.4 RS: ~~Contribution~~Influence of feature interactions

Strong pairwise interactive effects are found between MLH vs. time since last precipitation and MLH vs. maximum wind speed and shown in Figs 8a and 8b. SHAP interaction effects between MLH and time since last precipitation are most pronounced for MLHs below $\sim$ 500 m agl (Fig. 8a). Interaction values are negative for low MLHs paired with time since last precipitation close to zero hours. With increasing time since last precipitation, interaction effects become positive, thus increasing the contribution of Tprec and MLH to the model outcome. An explanation of this pattern concerning underlying processes could be that due to the lack of precipitation, a higher number of particles is available in the atmosphere for accumulation, hence increasing the accumulation effect of a shallow MLH. In case of recent precipitation, the accumulation effect of a shallow MLH is weakened. For higher MLHs, interactive effects with time since the last precipitation event are marginal. Interactive effects between MLH and wind speed are shown in Fig. 8b. Positive SHAP values for maximum wind speeds below $\sim$2 m/s reflect stable situations, favoring the accumulation of particles, whereas high wind speeds enhance the ventilation of particles (Sujatha et al., 2016). This can also be deduced from Fig. 8b, which shows increased SHAP values for low wind speeds in combination with a low MLH. Low wind speeds combined with a high MLH ($>\sim$1000 m agl), on the other hand, result in decreased SHAP values. Similarly, low MLHs combined with higher wind speeds ($>\sim$2 m/s) also decrease predictions of total PM_1 concentrations. Maximum wind speed and time since last precipitation (plot not shown here) interact in a similar way. The positive effect of low wind speeds on the model outcome is increasing with increasing time since last precipitation.

4.3 Meteorological conditions of high-pollution events

To further identify conditions that favor high pollution episodes, the data set is split into situations with exceptionally high total PM_1 concentrations (>95th percentile) and situations with typical concentrations of total PM_1 (interquartile range, IQR). This is done for the meteorological summer and winter seasons to contrast dominant drivers between these seasons. Mean SHAP values refer to the total PM_1 model, corresponding input feature distributions and species fractions for the two subgroups are aggregated seasonally. This allows for a quantification of seasonal feature contributions to average or polluted situations.

Figs 9 & 10 show mean SHAP values for typical (left) and high-pollution (right) situations in the upper panel. The distribution of SHAP values are shown as box plots for each feature. Absolute feature value distributions are given in the bottom of the figure. In the lowest subpanel, the chemical composition of the total PM_1 concentration for each subgroup is shown. The

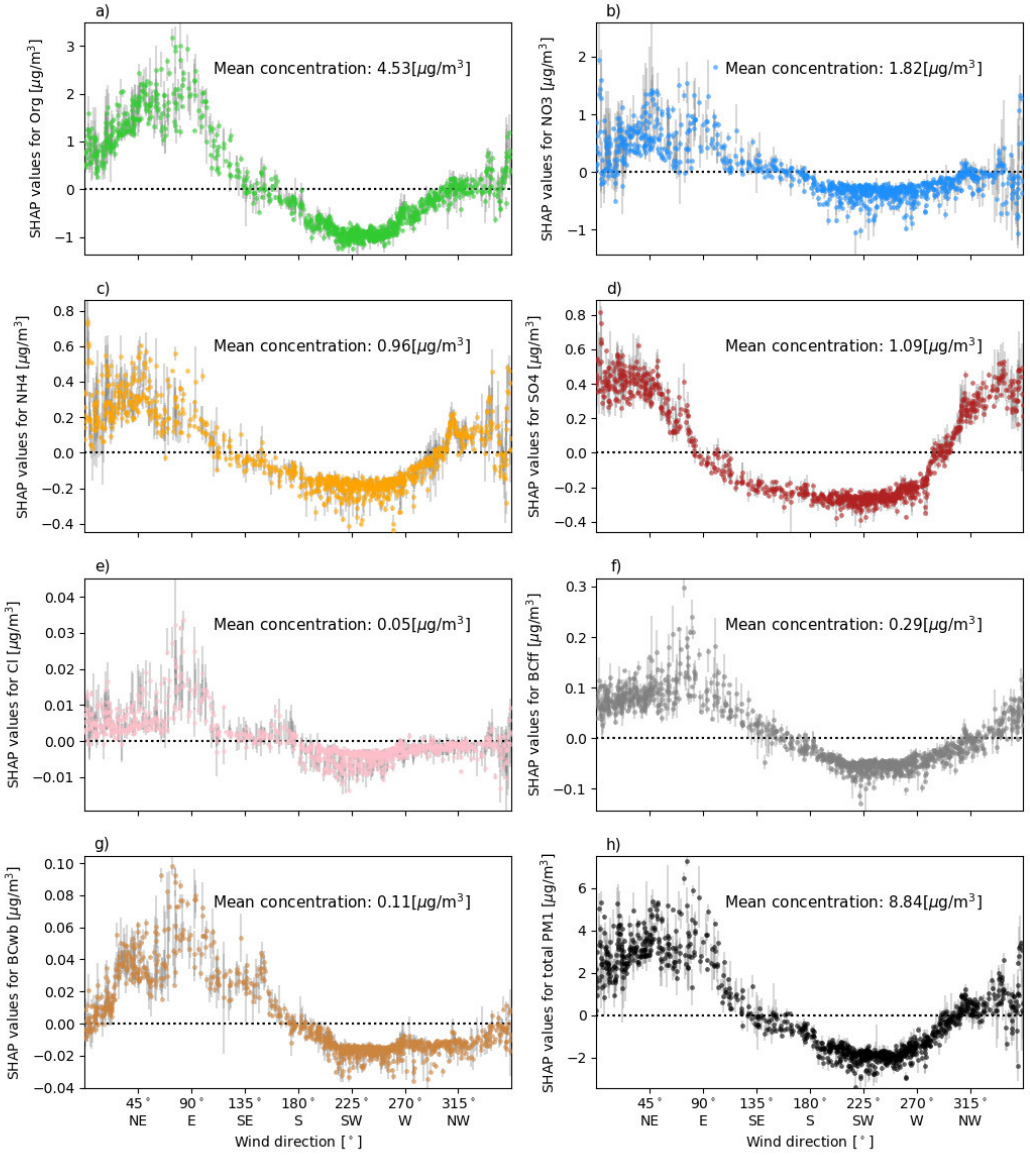

Figure 7. As Fig. 5 for wind direction SHAP values (contribution of 3-day mean wind direction to the prediction of species and total PM_1 for each data instance) vs. absolute wind direction [°].

largest contributor to high pollution situations in winter is air temperature (Fig. 9). SHAP values for temperature are substantially increased during high pollution situations, when temperatures are systematically lower. Further contributing factors to high pollution situations are the lows MLHs, low wind speeds, a high average NO_3^- fraction of the previous day and negative u (i.e., winds from the east) and v (i.e., winds from the north) wind components. In winter, the PM_1 composition shows a

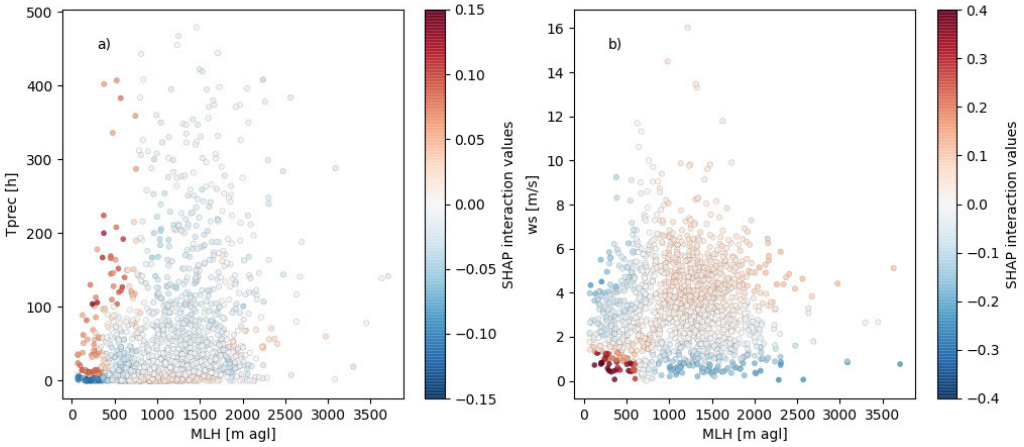

Figure 8. MLH vs. a) time since last precipitation and MLH vs. b) maximum wind speed, respectively, colored by the SHAP interaction values for the respective features.

Table 1. Statistics for typical PM_1 concentrations (mean, median, IQR) and high-pollution concentrations (>95th percentile).

PM1 concentrations	Mean	Median	Interquartile range	95th percentile
Winter (DJF)	11.1 μg/m^3	6.3 μg/m^3	2.7-15.4 μg/m^3	34.3 μg/m^3
Summer (JJA)	7.5 μg/m^3	6.0 μg/m^3	3.5-10.1 μg/m^3	18.2 μg/m^3

relatively large fraction of nitrates, which is increased during high pollution situations (Fig. 9, lower panel). High concentrations of nitrate in winter can be linked to advection or to enhanced formation due to the temperature-dependent low volatility of ammonium nitrate (Petetin et al., 2014). The organic matter fraction is slightly decreased during high pollution situations. MLH and maximum wind speed RS: ~~contributions to~~ influences on high pollution situations are linked to low ventilation conditions which are very frequent in winter (Dupont et al., 2016). Positive RS: ~~contributions~~ influences of wind direction for inflow from the northern and eastern sectors are dominant during high pollution situations while inflow from the southern and western sectors prevails during average pollution situations (see Fig. 7, Bressi et al., 2013; Petetin et al., 2014; Srivastava et al., 2018). Note that the time since the last precipitation is increased during high pollution situations, but the effects on the model outcome is weak. This suggests that lacking precipitation is not a direct driver of modelled total PM_1 concentrations, but increases the contribution of other input features (see Fig. 8a) or is a meaningful factor in only some situations.

Summer total PM_1 composition (Fig. 10) is characterised by a larger fraction of organics compared to the winter season (Fig. 9). As a considerable fraction of organic matter is formed locally (Petetin et al., 2014), the increased proportion of organics could be due to more frequent stagnant synoptic situations that may limit the advection of transported SIA particles. In addition, the positive SHAP values of solar irradiation and temperature highlight that the solar irradiation stimulates transformation pro-

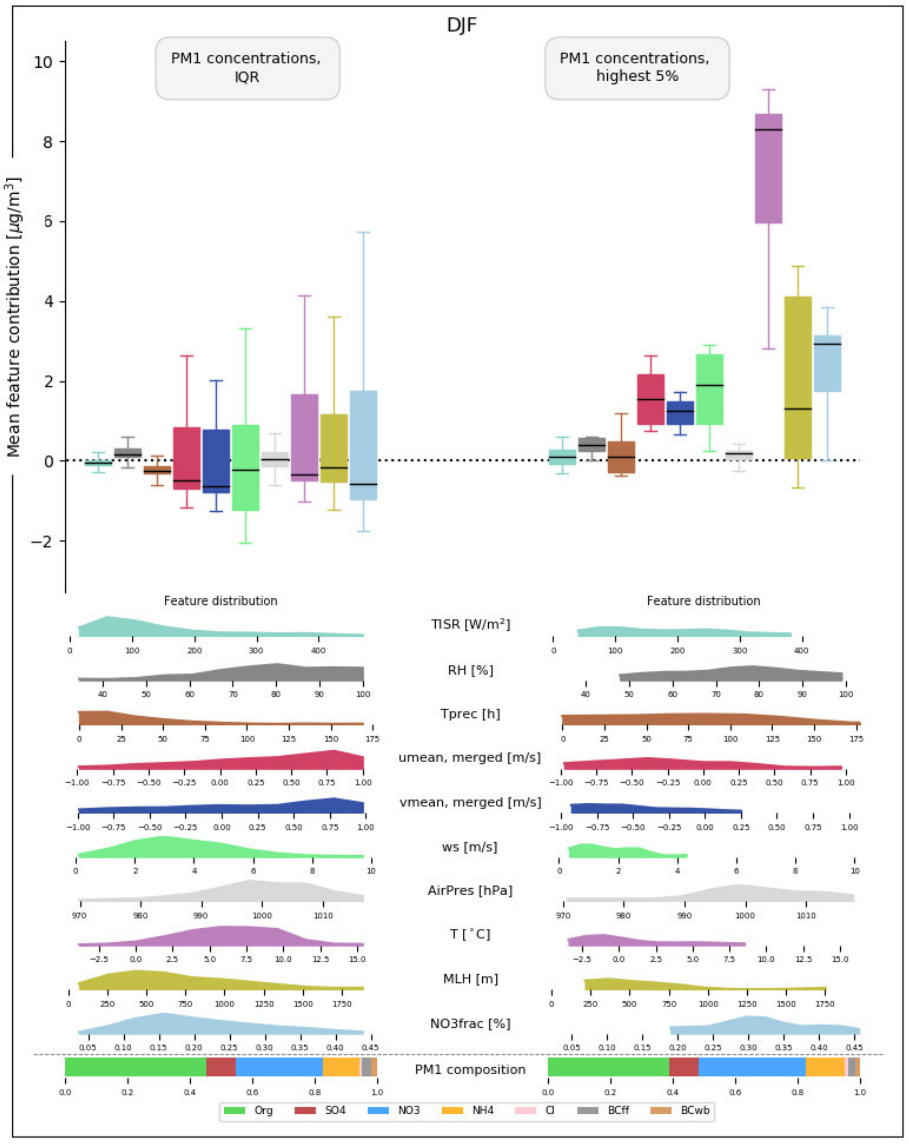

Figure 9. Mean feature contributions (i.e., SHAP values) for situations with low total PM_1 concentrations (left) and situations with high pollution (right), respectively, during winter (December, January, February). Respective range of SHAP values by species are shown as box plots, with median (bold line), 25-75th percentile range (boxes), and 10–90th percentile range (whiskers). Both training and test data are included. Absolute feature value distributions (given as normalised frequencies) as well as the chemical composition of the total PM_1 concentration are shown in the subpanels. Colors of the box plots correspond to colors in the feature distribution subpanels. SHAP values of the input features u_norm_3d and u_norm as well as v_norm_3d and v_norm were merged to u_norm, merged and v_norm, merged to achieve better transparency.

cesses and increases the number of biogenic SOA particles (Guenther et al., 1993; Petetin et al., 2014). As mean temperatures are highest in summer, positive temperature SHAP values are associated with increased organic matter concentrations (Fig. 5). The higher importance (i.e. higher SHAP values) of time since the last precipitation event during high pollution situations points to an accumulation of particles in the atmosphere. Dry situations can also enhance the emission of dust over dry soils (Hoffmann and Funk, 2015). The negative RS: ~~contributions~~influences of MLH during both typical and high pollution situations reflects seasonality, as afternoon MLHs in summer are usually too high to have a substantial positive impact on total PM_1 concentrations (see Fig. 6). MLH is thus not expected to be a driver of day-to-day variations of summer total PM_1 concentrations. Note that the average MLH is higher during high pollution situations, which likely points to increased formation of SO_4^{2-} (see Fig. 6).

4.4 Day-to-day variability of selected pollution events

Analysing the combination of SHAP values of the various input features on a daily basis allows for direct attribution of the respective implications for modelled total PM_1 concentrations (Lundberg et al., 2020). Here, four particular pollution episodes are selected to analyse the model outcome with respect to physical processes (Figs 11-14). The examples highlight the advantages but also the limitations of the interpretation of the statistical model results. The high pollution episodes took place in winter 2016 (10th - 30th January and 25th November - 25th December), spring 2015 (11th - 31st March) and summer 2017 (8th - 28th June). The upper panels in Figs 13-16 indicate the total PM_1 prediction as horizontal black line with vertical black lines denoting the range of predictions of all 10 models. The observed species concentrations are shown in the corresponding colors. The subsequent panels show absolute values and SHAP values for the most relevant meteorological input features.

4.4.1 January 2016

Prior to the onset of the high-pollution episode in January 2016 (Fig. 11), the situation is characterised by MLHs in the range of 1000m, temperatures above freezing (∼5-10°C), frequent precipitation and winds from the southwest. The organic matter fraction dominates the particle speciation. The episode itself is reproduced well by the model. According to the model results, the event is largely temperature-driven, i.e. SHAP values of temperature explain a large fraction of the total PM_1 concentration variation (note the adjusted y-axis of the temperature SHAP values). On 18th January, temperatures drop below freezing, coupled with a decrease in MLH. As a consequence, both modelled and observed PM_1 concentrations start to rise. A further increase in total PM_1 concentrations is driven by a sharp transition from stronger southwestern to weaker northeastern winds (strong negative u component, weak negative v component) on January 19th. The combined effects of these changes lead to a marked increase in total RS: modelled PM_1 concentrations, peaking at $\sim 37\,\mu g/m^3$ on 20th January. On the following days, temperatures increase steadily, thus the contribution of temperature decreases. At the same time, although values of MLH remain almost constant, the contribution of MLH drops substantially from $\sim 5\,\mu g/m^3$ to $\sim 2\,\mu g/m^3$. This is due to interactive effects between MLH and the features wind speed, time since last precipitation and normalised v-wind-component. All of these features increase the contribution of MLH on 20th January, but decrease its contribution on 21st-23rd January. RS: The physical explanation behind this pattern would be that lacking wet deposition and low wind speeds increase particle numbers

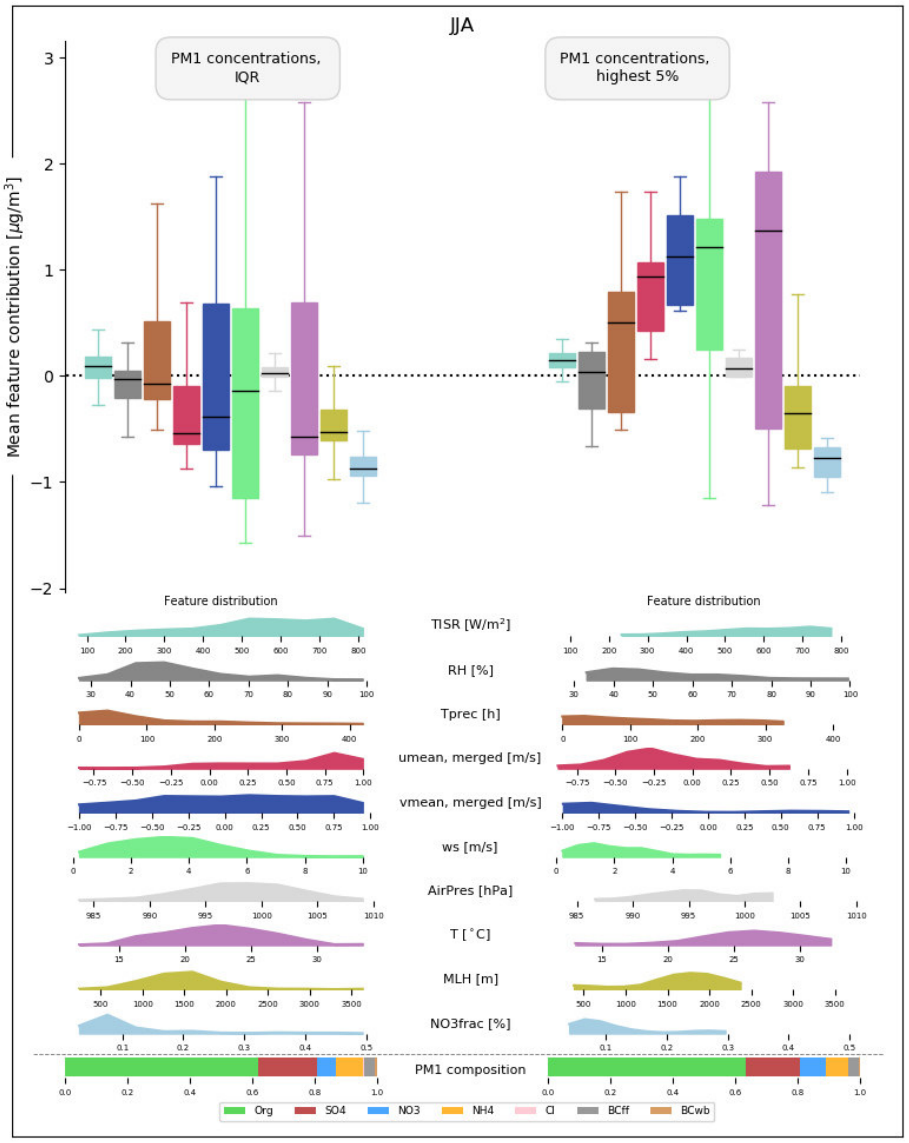

Figure 10. As Fig. 9 for mean feature contributions (i.e., SHAP values) for situations with low total PM_1 concentrations (left) and situations with high pollution (right), respectively, during summer (July, June, August).

405 in the atmosphere, while inflow from northeasterly directions increase particle numbers in the atmosphere. Given that there is now a large number of particles present, the accumulation effect of a low MLH is more efficient. The high pollution episode ceases after a shift to southeastern winds and the increasing temperatures. The pollution episode is characterised by a relatively large fraction of NO_3^- and NH_4^+, which explains the strong feature contribution of temperature to the modeled total PM_1 concentration, as the abundance of these species is temperature dependent (see Fig. 5) and points to a large contribution of

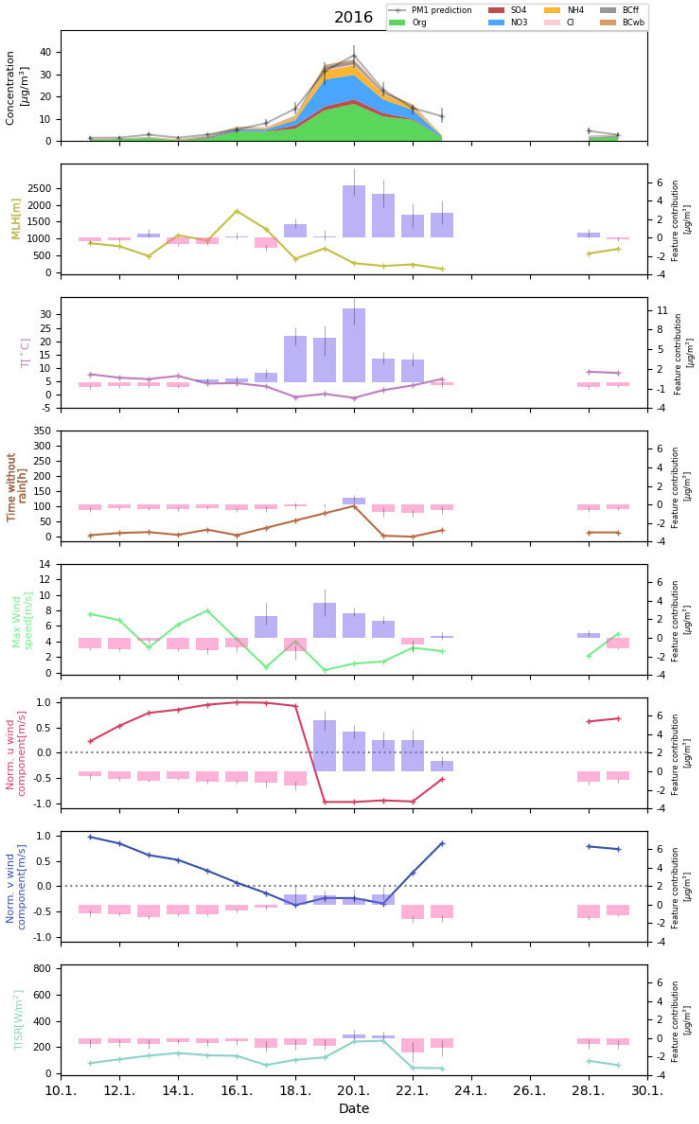

Figure 11. Winter pollution episode in January 2016. (a): predicted total PM_1 and observed PM_1 species concentrations, with absolute input feature values and corresponding SHAP values of (b) MLH, (c) temperature, (d) hours after rain, (e) maximum wind speed (f) normalised u wind and (g) normalised v wind component.

410 locally formed inorganic particles. Still, the contribution of wind direction and speed also suggests that advected secondary particles and their build-up in the boundary layer are relevant factors during the development of the high pollution episode (Petetin et al., 2014; Petit et al., 2014; Srivastava et al., 2018).

4.4.2 December 2016

A high-pollution episode with several peaks of total PM_1 is observed in November and December 2016. The first peak on 26th December is followed by an abrupt minimum in total PM_1 concentrations on 28th November, and a build-up of pollution in a shallow boundary layer towards the second peak on 2nd December with total PM_1 concentrations exceeding 40 $\mu g/m^3$. In the following days, total PM_1 concentrations continuously decrease, eventually reaching a second minimum on 11th December. A gradual increase in total PM_1 concentrations follows, resulting in a third (double-)peak total PM_1 concentration on 17th December. Total PM_1 concentrations drop to lower levels afterwards. Throughout the 3.5 week-long episode, high pollution is largely driven by shallow MLH (<∼500m), and weak north-northeasterly winds, i.e. a regime of low ventilation associated with high pressure conditions favorable for emission accumulation. During the brief periods with lower total PM_1 concentrations, these conditions are disrupted by a higher MLH (∼28th November), or a change in prevailing winds (∼11th December). In contrast to the pollution episode in January 2016, this December 2016 episode is not driven by temperature changes. Temperatures range between ∼5-12°C and have a minor RS: ~~contribution to~~ influence on to predicted total PM_1 concentrations (see also Fig. 5), emphasizing the different processes causing air pollution in the Paris region. Note that the model is not able to fully reproduce the pollution peak on December 2nd, which may be indicative of missing input features in the model. Judging from the PM_1 species composition during this time (relatively high fraction of NO_3^- and BC), it seems likely that missing information on particle emissions may be the reason for the difference between modeled and observed total PM_1 concentration.

4.4.3 June 2017

A period of above average total PM_1 concentrations occurred in June 2017. The episode is very well reproduced by the model, suggesting a strong dependence of the observed total PM_1 concentration to meteorological drivers. Although absolute total PM_1 concentrations are substantially lower than during the previously described winter pollution episodes, the event is still above average for summer pollution levels. Organic matter particles dominate the PM_1 fraction throughout the episode, with a relatively high SO_4^{2-} fraction. Conditions during this episode are characterised by strong solar irradiation (positive SHAP values) and high MLHs (mostly negative SHAP values), which show low day-to-day variability and reflect characteristic summer conditions. A lack of precipitation (no rain for a period of more than 2 weeks) and high temperatures also contribute to the total PM_1 concentrations during this episode. While solar irradiation and time since last precipitation are associated with positive SHAP values throughout this period, air temperature only has a positive contribution when exceeding ∼25 °C. This aligns with patterns shown in Fig. 5, where increased concentrations of organic matter and SO_4^{2-} are identified for high temperatures. Peak total PM_1 concentrations of ∼17 $\mu g/m^3$ are observed on June 20th and 21st. A change in the east-west wind component from western to eastern inflow directions in conjunction with an increase in temperatures to above 30 °C are the drivers of the modeled peak in total PM_1 concentrations. MLH is also increased with values ∼2000 m agl, which are associated with slightly positive SHAP values. This observation fits with findings described in section 4.2.2 and is likely linked to enhanced secondary particle formation (Megaritis et al., 2014; Jiang et al., 2019). As suggested by response patterns of species to changes in MLH shown in Fig. 7, this effect is linked to an increase in SO_4^{2-} concentrations. The main fraction of

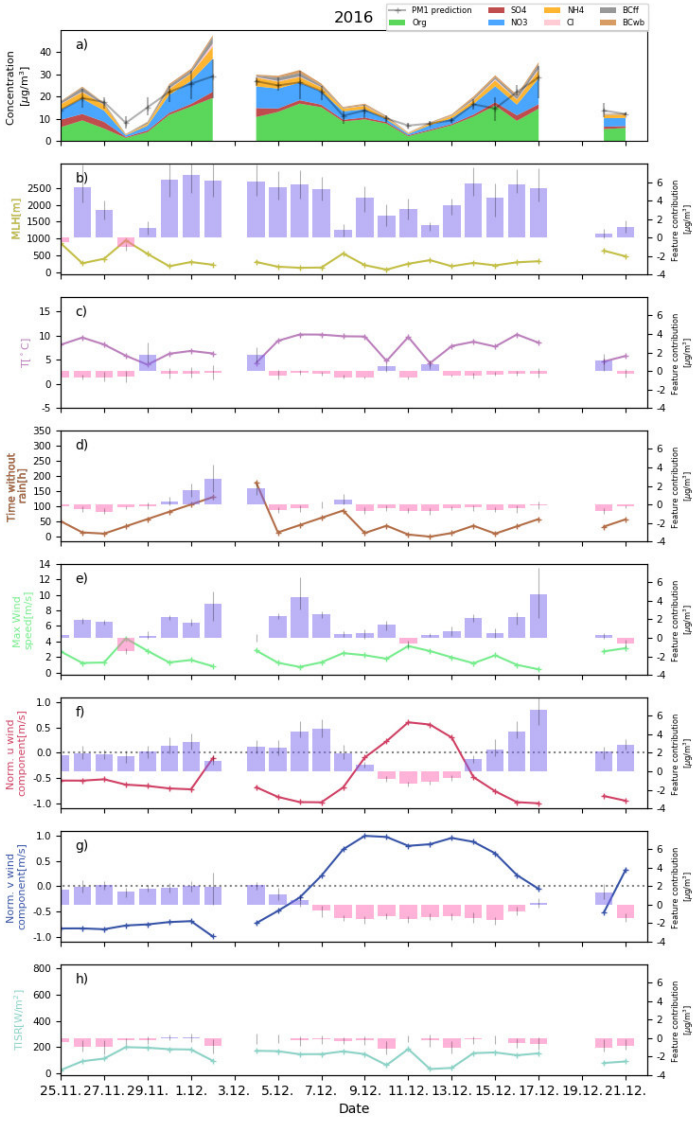

Figure 12. As Fig. 11 for a further winter pollution episode in December 2016.

the peak total PM_1 values, however, is linked to an increase in organic matter concentrations due to the warm temperatures (see Fig. 5).

4.4.4 March 2015

High particle concentrations are measured in early March 2015 with high day-to-day variability. This modelled course of the pollution episode is chosen to compare results to previous studies focusing on the evolution of this episode (Petit et al., 2017;

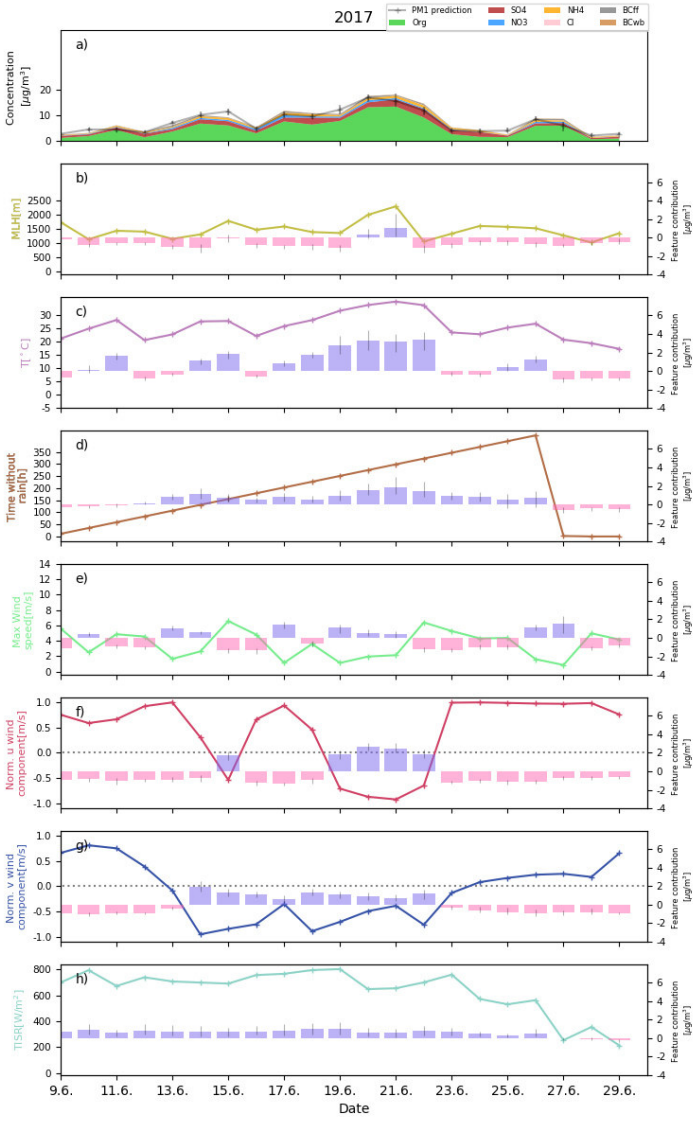

Figure 13. As Fig. 11 for an exemplary summer pollution episode in June 2017.

Srivastava et al., 2018). The episode is characterised by high fractions of SIA particles, in particular SO_4^{2-}, NH_4^+ and NO_3^- (Fig. 14, upper panel) and similar concentrations observed at multiple measurement sites in France (Petit et al., 2017). Contributions of local sources are low and much of the episode is characterised by winds blowing in from the northwest, advecting aged SIA particles (Petit et al., 2017; Srivastava et al., 2018) and organic particles of secondary origin (Srivastava et al., 2019) towards SIRTA. A widespread scarcity of rain probably enhanced the large-scale formation of secondary pollution across western Europe (in particular western Germany, The Netherlands, Luxemburg, Petit et al., 2017), which were then transported towards

SIRTA. This is reflected by the SHAP values of the u and v wind components, which are positive throughout the episode (see Fig. 14g & 14h). Concentration peaks of total PM_1 are measured on 18th and 20th March. Both peaks are characterised by a rapid development of total PM_1 concentrations. As described in Petit et al. (2017), these strong daily variations of total PM_1, which are mainly driven by the SIA fraction, could be due to varying synoptic cycles, especially the passage of cold fronts. The RS: ~~contribution~~influence of MLH and temperature is relatively small, which is consistent with the high influence of advection on total PM_1 concentrations during the episode. The exceptional character of the episode (see Petit et al., 2017) partly explains the bad performance of the model in capturing total PM_1 variability during the event. Unusual rain shortage is observed in large areas of Western Europe prior to the episode (Petit et al., 2017). While time since precipitation at the SIRTA-site is a large positive contributor to the model outcome (see Fig. 14d), it is not driving the day-to-day variations. The unusual nature of this event and lacking information on emission in the source regions and formation processes along air mass trajectories in the model likely explain why the model has difficulties in reproducing this pollution episode. While this has implications for the application of explainable machine learning models for rare events, this is not expected to be an issue for the other cases and seasonal results presented here.

5 Conclusions and outlook

In this study, dominant patterns of meteorological drivers of PM_1 species and total PM_1 concentrations are identified and analysed using a novel, data-driven RS: ~~statistical~~ approach. A machine learning model is set up to RS: ~~explain~~analyse measured speciated and total PM_1 concentrations based on meteorological measurements from the SIRTA supersite, southwest of Paris. The RS: ~~statistical~~machine learning model is able to reproduce daily variability of particle concentrations well, and is used to analyse and quantify the atmospheric processes causing high-pollution episodes during different seasons using a SHAP-value framework.RS: ~~Comparison of the results based on the machine learning model with findings of previous studies on air quality patterns in the Paris region shows good agreement.~~As interactions between the meteorological variables are accounted for, the model enables the separation, quantification and comparison of their respective impacts the individual events. It is shown that ambient meteorology can substantially exacerbate air pollution. RS: Results of this study point to the distinguished role of RS: ~~Peak concentrations of total PM_1 in winter are mainly driven by~~ shallow MLHs, low temperatures and low wind speeds RS: during peak PM_1 episodes in winter. These conditions are often amplified by northeastern wind inflow under high-pressure RS: ~~conditions~~synoptic circulation. A detailed analysis reveals RS: ~~different~~how the RS: meteorological drivers of RS: winter high-pollution episodes RS: ~~in winter~~interact. For an episode in January 2016, model results show a strong RS: ~~contribution~~influence of temperature to the elevated PM_1 concentrations during this episode (up to 11 $\mu g/m^3$ are attributed to temperature), suggesting enhanced local, temperature-dependent particle formation. During a different, prolonged pollution episode in December 2016, temperature levels were relatively stable and had no influence. Here, RS: ~~contributions of~~ MLH (<500 m asl) was quantified to be the main driver of RS: modelled PM_1 peak concentrations with contributions up to 6 $\mu g/m^3$, along with wind direction contributions of up to $\sim$6 $\mu g/m^3$. Total PM_1 concentrations in spring can be as high as 50 $\mu g/m^3$. These peaks in spring are not as well reproduced by the model as winter episodes and are likely due to new particle formation processes along the air mass trajectories, in particular of nitrate.

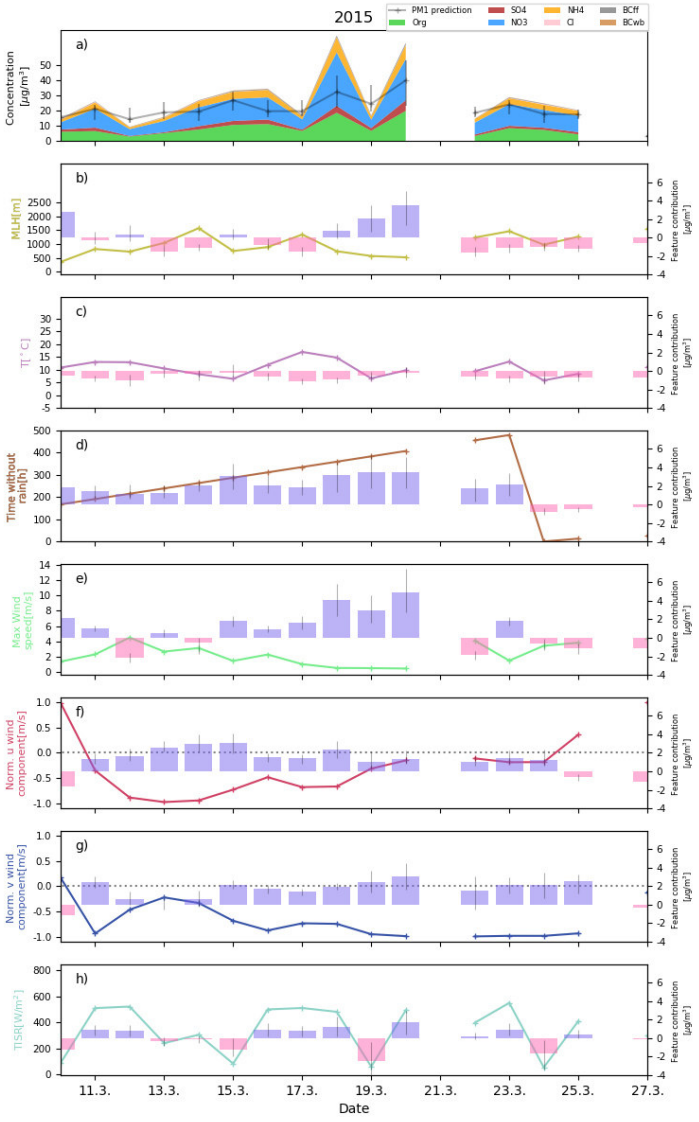

Figure 14. As Fig. 11 for an exemplary spring pollution episode in March 2015.

Summer PM_1 concentrations are lower than in other seasons. Model results suggest that summer peak concentrations are largely driven by high temperatures, particle advection from Paris and continental Europe with low wind speeds and prolonged periods without precipitation. For an example episode in June 2017, temperatures above 30°C contribute $\sim 3\,\mu g/m^3$ to the total PM_1 concentration. On site scarcity of rain increases air pollution, but does not appear to be a main driver of strong day-to-day variations in particle concentrations. Presumably, this is because droughts are synoptic and are spread over several days or even weeks. Thus, they present very low inter-daily variability on the local scale. Nonetheless, Petit et al. (2017) have

highlighted the link between extreme PM concentrations (especially during spring) and extreme precipitation deficit (compared to average conditions). Main drivers of day-to-day variability of predicted PM_1 concentrations are changes in wind direction, air temperature and MLH. These changes often superimpose the influence of time without precipitation. Individual PM_1 species are shown to respond differently to changes in temperature. While SO_4^{2-} and organic matter concentrations are increased during both high and low temperature situations, NH_4^+ and NO_3^- are substantially increased only at low temperatures. Model results indicate that SIA particle formation is enhanced during shallow MLH conditions.

Many of the results presented here hold true for regions other than RS: ~~suburban Paris~~the Sirta supersite and are thus beneficial for the general understanding of drivers of air pollution. This includes the RS: nonlinear response of PM_1 concentrations to changes in temperature or MLH, including their dependencies on other meteorological factors, which has potential implications for the settings of future CTMs. Furthermore, the temperature-dependency of PM_1 is relevant in terms of rising temperatures due to climate change RS: ~~importance of formation processes of secondary pollutants as well as the dominant role of the MLH for PM_1 concentrations~~. The RS: ~~contribution~~importance of wind direction highlights the role of advected pollution and emphasizes the need for large-scale measures against air pollution. RS: ~~The GBRT approach in combination with the SHAP regression values presented here provides an intuitive tool to assess meteorological drivers of air pollution and to advance the understanding of high pollution events by uncovering different physical mechanisms leading to high-pollution episodes.~~ RS: ~~To our knowledge, this is the first time that the SHAP-framework for explainable machine learning is applied in atmospheric sciences~~.

RS: For policy makers, the presented approach could prove beneficial in multiple ways for air quality policies. Preventative warnings could be issued to the public if the identified meteorological conditions exacerbating air pollution are to be expected. RS: ~~The results of this study are highly relevant for policy makers, e.g. by providing a basis for future clean air programs or by providing the potential of a statistically-based early warning system for high pollution episodes. Statistical~~ RS: Another potential future application could be the attribution of changes in air quality to policy measures RS: by comparing an "expected" level of air pollution under given meteorological conditions to actual observations (e.g., Cermak and Knutti, 2009),RS: ~~and may help~~ which may help political decision makers develop and implement effective clean-air policies. Future efforts could also combine the statistical model framework with short-term weather forecasts, which would allow to provide an air quality forecast based on the predictions of the statistical models, taking into account expected meteorological conditions. This study could be extended in the future, e.g. by including information on anthropogenic emissions or further stations down- and upwind of SIRTA, which would allow further analysis of dominant advection patterns. Furthermore, information on emissions or meteorology in the source region of air masses e.g., using satellite-based observations, might be helpful to better reproduce particle transport patterns. This could be complemented by incorporating synoptic variables, e.g., the North Atlantic Oscillation (NAO) index.

Data availability. SIRTA-ReOBS data can be accessed online (https://sirta.ipsl.fr/reobs.html), ACSM data are available upon request.

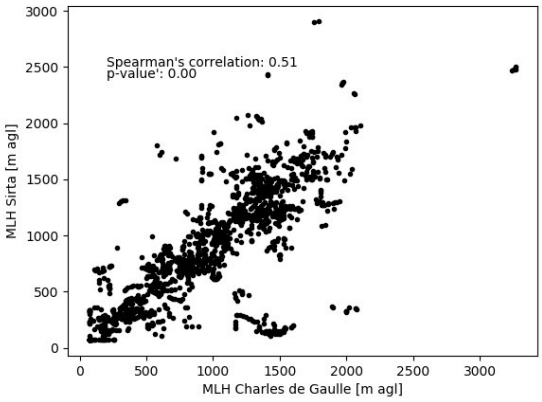

Figure A1. Scatterplot for MLH [m agl] measured at Sirta vs. MLH measured at Charles de Gaulle airport .

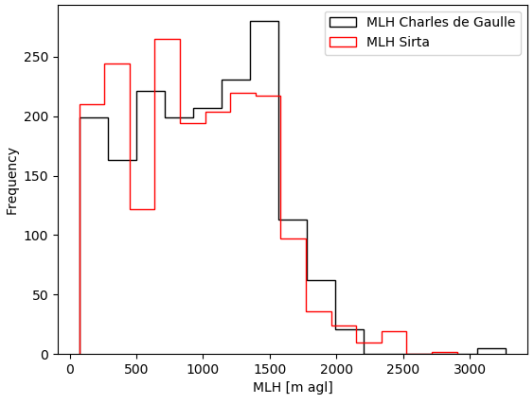

Figure A2. Histogram showing the frequency of occurrence for MLH [m agl] measured at Sirta (red) vs. MLH measured at Charles de Gaulle airport (black).

Appendix A: Comparison of mixed layer height (MLH) measured at Sirta and Charles de Gaulle airport

As mentioned in section 2.2, ca. 90 missing MLH values in 2016 were replaced with measurements conducted at the Charles de Gaulle airport (see Fig. 1). Figs A2 and A1 summarize MLH values for 2016 when measurements from both sites are available (afternoon period). As shown in Fig. A1, measurements at both sites generally agree well, except for some outliers. Spearman's rank coefficient is significant (p-value < 0.05) and has a value of 0.51.

A comparison of the frequency of occurrence is shown as histogram in Fig. A1 and indicates good agreement as well.

Author contributions. Conceptualization, R.S., J.C., M.H., S.K.; Data acquisition, J.-E.P., O.F., M.H., and S.K.; Formal analysis, R.S; Investigation, R.S.; Methodology, R.S., J.C., M.H., S.K, H.A., J.F. and M.K.; Visualization, R.S.; Writing-original draft, R.S.; Writing-review & editing, R.S., J.C., M.H., S.K, J.F., H.A., J.-E.P., O.F., and M.K.

Competing interests. The authors declare that they have no conflict of interest.

Acknowledgements. The authors would like to acknowledge the ACTRIS-2 project that received funding from the European Union's Horizon 2020 research and innovation programme under grant agreement No 654109. Acknowledgements are extended to Rodrigo Guzman and Christophe Boitel for providing the latest update of the SIRTA ReOBS dataset. Furthermore, the authors acknowledge Scott Lundberg for his work on the TreeSHAP algorithm. R.S. was supported by the KIT Graduate School for Climate and Environment (GRACE).

References

Baklanov, A., Molina, L. T., and Gauss, M.: Megacities, air quality and climate, Atmos. Environ., 126, 235–249, https://doi.org/10.1016/j.atmosenv.2015.11.059, https://linkinghub.elsevier.com/retrieve/pii/S1352231015305665, 2016.

Beekmann, M., Prévôt, A. S., Drewnick, F., Sciare, J., Pandis, S. N., Denier Van Der Gon, H. A., Crippa, M., Freutel, F., Poulain, L., Ghersi, V., Rodriguez, E., Beirle, S., Zotter, P., Von Der Weiden-Reinmüller, S. L., Bressi, M., Fountoukis, C., Petetin, H., Szidat, S., Schneider, J., Rosso, A., El Haddad, I., Megaritis, A., Zhang, Q. J., Michoud, V., Slowik, J. G., Moukhtar, S., Kolmonen, P., Stohl, A., Eckhardt, S., Borbon, A., Gros, V., Marchand, N., Jaffrezo, J. L., Schwarzenboeck, A., Colomb, A., Wiedensohler, A., Borrmann, S., Lawrence, M., Baklanov, A., and Baltensperger, U.: In situ, satellite measurement and model evidence on the dominant regional contribution to fine particulate matter levels in the Paris megacity, Atmos. Chem. Phys., 15, 9577–9591, https://doi.org/10.5194/acp-15-9577-2015, 2015.

Bressi, M., Sciare, J., Ghersi, V., Bonnaire, N., Nicolas, J. B., Petit, J. E., Moukhtar, S., Rosso, A., Mihalopoulos, N., and Féron, A.: A one-year comprehensive chemical characterisation of fine aerosol (PM2.5) at urban, suburban and rural background sites in the region of Paris (France), Atmos. Chem. Phys., 13, 7825–7844, https://doi.org/10.5194/acp-13-7825-2013, 2013.

Bressi, M., Sciare, J., Ghersi, V., Mihalopoulos, N., Petit, J. E., Nicolas, J. B., Moukhtar, S., Rosso, A., Féron, A., Bonnaire, N., Poulakis, E., and Theodosi, C.: Sources and geographical origins of fine aerosols in Paris (France), Atmos. Chem. Phys., 14, 8813–8839, https://doi.org/10.5194/acp-14-8813-2014, 2014.

Cermak, J. and Knutti, R.: Beijing Olympics as an aerosol field experiment, Geophys. Res. Lett., 36, L10 806, https://doi.org/10.1029/2009GL038572, http://doi.wiley.com/10.1029/2009GL038572, 2009.

Chafe, Z. A., Brauer, M., Klimont, Z., Van Dingenen, R., Mehta, S., Rao, S., Riahi, K., Dentener, F., and Smith, K. R.: Household Cooking with Solid Fuels Contributes to Ambient PM 2.5 Air Pollution and the Burden of Disease, Environ. Health Perspect., 122, 1314–1320, https://doi.org/10.1289/ehp.1206340, https://ehp.niehs.nih.gov/doi/10.1289/ehp.1206340, 2014.

Chen, G., Li, S., Zhang, Y., Zhang, W., Li, D., Wei, X., He, Y., Bell, M. L., Williams, G., Marks, G. B., Jalaludin, B., Abramson, M. J., and Guo, Y.: Effects of ambient PM1 air pollution on daily emergency hospital visits in China: an epidemiological study, Lancet Planet. Heal., 1, e221–e229, https://doi.org/10.1016/S2542-5196(17)30100-6, https://linkinghub.elsevier.com/retrieve/pii/S0160412018303866https://linkinghub.elsevier.com/retrieve/pii/S2542519617301006, 2017a.

Chen, G., Li, S., Zhang, Y., Zhang, W., Li, D., Wei, X., He, Y., Bell, M. L., Williams, G., Marks, G. B., Jalaludin, B., Abramson, M. J., and Guo, Y.: Effects of ambient PM 1 air pollution on daily emergency hospital visits in China: an epidemiological study, Lancet Planet. Heal., 1, e221–e229, https://doi.org/10.1016/S2542-5196(17)30100-6, http://dx.doi.org/10.1016/S2542-5196(17)30100-6https://linkinghub.elsevier.com/retrieve/pii/S2542519617301006, 2017b.

Chen, Y., Schleicher, N., Chen, Y., Chai, F., and Norra, S.: The influence of governmental mitigation measures on contamination characteristics of PM2.5 in Beijing, Sci. Total Environ., 490, 647–658, https://doi.org/10.1016/j.scitotenv.2014.05.049, http://dx.doi.org/10.1016/j.scitotenv.2014.05.049https://linkinghub.elsevier.com/retrieve/pii/S0048969714007268, 2014.

Cheng, Y., Zheng, G., Wei, C., Mu, Q., Zheng, B., Wang, Z., Gao, M., Zhang, Q., He, K., Carmichael, G., Pöschl, U., and Su, H.: Reactive nitrogen chemistry in aerosol water as a source of sulfate during haze events in China, Sci. Adv., 2, e1601 530, https://doi.org/10.1126/sciadv.1601530, http://advances.sciencemag.org/lookup/doi/10.1126/sciadv.1601530, 2016.

Chiriaco, M., Dupont, J.-C., Bastin, S., Badosa, J., Lopez, J., Haeffelin, M., Chepfer, H., and Guzman, R.: ReOBS: a new approach to synthesize long-term multi-variable dataset and application to the SIRTA supersite, Earth Syst. Sci. Data, 10, 919–940, https://doi.org/10.5194/essd-10-919-2018, https://www.earth-syst-sci-data.net/10/919/2018/, 2018.

Churkina, G., Kuik, F., Bonn, B., Lauer, A., Grote, R., Tomiak, K., and Butler, T. M.: Effect of VOC Emissions from Vegetation on Air Quality in Berlin during a Heatwave, Environ. Sci. Technol., 51, 6120–6130, https://doi.org/10.1021/acs.est.6b06514, http://pubs.acs.org/doi/abs/10.1021/acs.est.6b06514, 2017.

Clegg, S. L., Brimblecombe, P., and Wexler, A. S.: Thermodynamic Model of the System H^+ - $NH_4{}^+$ - Na^+ - $SO_4{}^{2-}$ - NO_{3-} - Cl^- -H_2O at 298.15 K, J. Phys. Chem. A, 102, 2155–2171, https://doi.org/10.1021/jp973043j, https://pubs.acs.org/doi/10.1021/jp973043j, 1998.

Dawson, J. P., Adams, P. J., and Pandis, S. N.: Sensitivity of PM2.5 to climate in the Eastern US: a modeling case study, Atmos. Chem. Phys., 7, 4295–4309, https://doi.org/10.5194/acp-7-4295-2007, http://www.atmos-chem-phys.net/7/4295/2007/, 2007.

Dey, S., Caulfield, B., and Ghosh, B.: Potential health and economic benefits of banning diesel traffic in Dublin, Ireland, J. Transp. Heal., 10, 156–166, https://doi.org/10.1016/j.jth.2018.04.006, https://linkinghub.elsevier.com/retrieve/pii/S1352231018301158https://linkinghub.elsevier.com/retrieve/pii/S2214140517307740, 2018.

Drinovec, L., Močnik, G., Zotter, P., Prévôt, A. S., Ruckstuhl, C., Coz, E., Rupakheti, M., Sciare, J., Müller, T., Wiedensohler, A., and Hansen, A. D.: The "dual-spot" Aethalometer: An improved measurement of aerosol black carbon with real-time loading compensation, Atmos. Meas. Tech., 8, 1965–1979, https://doi.org/10.5194/amt-8-1965-2015, 2015.

Dupont, J.-C., Haeffelin, M., Badosa, J., Elias, T., Favez, O., Petit, J., Meleux, F., Sciare, J., Crenn, V., and Bonne, J.: Role of the boundary layer dynamics effects on an extreme air pollution event in Paris, Atmos. Environ., 141, 571–579, https://doi.org/10.1016/j.atmosenv.2016.06.061, http://linkinghub.elsevier.com/retrieve/pii/S1352231016304940, 2016.

Elith, J., Leathwick, J. R., and Hastie, T.: A working guide to boosted regression trees, J. Anim. Ecol., 77, 802–813, https://doi.org/10.1111/j.1365-2656.2008.01390.x, http://doi.wiley.com/10.1111/j.1365-2656.2008.01390.x, 2008.

Ervens, B., Turpin, B. J., and Weber, R. J.: Secondary organic aerosol formation in cloud droplets and aqueous particles (aqSOA): a review of laboratory, field and model studies, Atmos. Chem. Phys., 11, 11 069–11 102, https://doi.org/10.5194/acp-11-11069-2011, https://www.atmos-chem-phys.net/11/11069/2011/, 2011.

Favez, O., Cachier, H., Sciare, J., Sarda-Estève, R., and Martinon, L.: Evidence for a significant contribution of wood burning aerosols to PM2.5 during the winter season in Paris, France, Atmos. Environ., 43, 3640–3644, https://doi.org/10.1016/j.atmosenv.2009.04.035, 2009.

Fowler, D., Pilegaard, K., Sutton, M., Ambus, P., Raivonen, M., Duyzer, J., Simpson, D., Fagerli, H., Fuzzi, S., Schjoerring, J., Granier, C., Neftel, A., Isaksen, I., Laj, P., Maione, M., Monks, P., Burkhardt, J., Daemmgen, U., Neirynck, J., Personne, E., Wichink-Kruit, R., Butterbach-Bahl, K., Flechard, C., Tuovinen, J., Coyle, M., Gerosa, G., Loubet, B., Altimir, N., Gruenhage, L., Ammann, C., Cieslik, S., Paoletti, E., Mikkelsen, T., Ro-Poulsen, H., Cellier, P., Cape, J., Horváth, L., Loreto, F., Niinemets, Ü., Palmer, P., Rinne, J., Misztal, P., Nemitz, E., Nilsson, D., Pryor, S., Gallagher, M., Vesala, T., Skiba, U., Brüggemann, N., Zechmeister-Boltenstern, S., Williams, J., O'Dowd, C., Facchini, M., de Leeuw, G., Flossman, A., Chaumerliac, N., and Erisman, J.: Atmospheric composition change: Ecosystems–Atmosphere interactions, Atmos. Environ., 43, 5193–5267, https://doi.org/10.1016/j.atmosenv.2009.07.068, https://linkinghub.elsevier.com/retrieve/pii/S1352231009006633, 2009.

Friedman, J. H.: Greedy Function Approximation: A Gradient Boosting Machine, Ann. Stat., 29, 1189–1232, https://doi.org/10.1214/aos/1013203451, http://projecteuclid.org/euclid.aos/1013203451, 2001.

Friedman, J. H.: Stochastic gradient boosting, Comput. Stat. Data Anal., 38, 367–378, https://doi.org/10.1016/S0167-9473(01)00065-2, http://linkinghub.elsevier.com/retrieve/pii/S0167947301000652, 2002.

Fuchs, J., Cermak, J., and Andersen, H.: Building a cloud in the Southeast Atlantic: Understanding low-cloud controls based on satellite observations with machine learning, Atmos. Chem. Phys. Discuss., 2, 1–23, https://doi.org/10.5194/acp-2018-593, https://www.atmos-chem-phys-discuss.net/acp-2018-593/, 2018.

Geiß, A., Wiegner, M., Bonn, B., Schäfer, K., Forkel, R., Von Schneidemesser, E., Münkel, C., Lok Chan, K., and Nothard, R.: Mixing layer height as an indicator for urban air quality?, Atmos. Meas. Tech., 10, 2969–2988, https://doi.org/10.5194/amt-10-2969-2017, 2017.

Gen, M., Zhang, R., Huang, D. D., Li, Y., and Chan, C. K.: Heterogeneous SO_2 Oxidation in Sulfate Formation by Photolysis of Particulate Nitrate, Environ. Sci. Technol. Lett., 6, 86–91, https://doi.org/10.1021/acs.estlett.8b00681, https://pubs.acs.org/doi/10.1021/acs.estlett.8b00681, 2019.

Goldstein, A., Kapelner, A., Bleich, J., and Pitkin, E.: Peeking Inside the Black Box: Visualizing Statistical Learning With Plots of Individual Conditional Expectation, J. Comput. Graph. Stat., 24, 44–65, https://doi.org/10.1080/10618600.2014.907095, http://www.tandfonline.com/doi/full/10.1080/10618600.2014.907095, 2015.

Grange, S. K., Carslaw, D. C., Lewis, A. C., Boleti, E., and Hueglin, C.: Random forest meteorological normalisation models for Swiss PM10 trend analysis, Atmos. Chem. Phys., 18, 6223–6239, https://doi.org/10.5194/acp-18-6223-2018, https://www.atmos-chem-phys.net/18/6223/2018/, 2018.

Guenther, A. B., Zimmerman, P. R., Harley, P. C., Monson, R. K., and Fall, R.: Isoprene and monoterpene emission rate variability: Model evaluations and sensitivity analyses, J. Geophys. Res., 98, 12 609–12 617, https://doi.org/10.1029/93JD00527, http://doi.wiley.com/10.1029/93JD00527, 1993.

Gupta, P. and Christopher, S. A.: Particulate matter air quality assessment using integrated surface, satellite, and meteorological products: Multiple regression approach, J. Geophys. Res., 114, D14 205, https://doi.org/10.1029/2008JD011496, http://doi.wiley.com/10.1029/2008JD011496, 2009.

Haeffelin, M., Bock, O., Boitel, C., Bony, S., Bouniol, D., Chepfer, H., Chiriaco, M., Cuesta, J., Drobinski, P., Flamant, C., Grall, M., Hodzic, A., Hourdin, F., Lapouge, F., Mathieu, A., Morille, Y., Naud, C., Pelon, J., Pietras, C., Protat, A., Romand, B., Scialom, G., and Vautard, R.: SIRTA, a ground-based atmospheric observatory for cloud and aerosol research, Ann. Geophys., 23, 253–275. <hal–00329 353>, 2005.

Healy, R. M., Sciare, J., Poulain, L., Kamili, K., Merkel, M., Müller, T., Wiedensohler, A., Eckhardt, S., Stohl, A., Sarda-Estève, R., McGillicuddy, E., O'Connor, I. P., Sodeau, J. R., and Wenger, J. C.: Sources and mixing state of size-resolved elemental carbon particles in a European megacity: Paris, Atmos. Chem. Phys., 12, 1681–1700, https://doi.org/10.5194/acp-12-1681-2012, https://www.atmos-chem-phys.net/12/1681/2012/, 2012.

Hennig, F., Quass, U., Hellack, B., Küpper, M., Kuhlbusch, T. A. J., Stafoggia, M., and Hoffmann, B.: Ultrafine and Fine Particle Number and Surface Area Concentrations and Daily Cause-Specific Mortality in the Ruhr Area, Germany, 2009–2014, Environ. Health Perspect., 126, 027 008, https://doi.org/10.1289/EHP2054, https://ehp.niehs.nih.gov/doi/10.1289/EHP2054, 2018.

Hoffmann, C. and Funk, R.: Diurnal changes of PM10-emission from arable soils in NE-Germany, Aeolian Res., 17, 117–127, https://doi.org/10.1016/j.aeolia.2015.03.002, http://dx.doi.org/10.1016/j.aeolia.2015.03.002, 2015.

Hu, X., Belle, J. H., Meng, X., Wildani, A., Waller, L. A., Strickland, M. J., and Liu, Y.: Estimating PM2.5 Concentrations in the Conterminous United States Using the Random Forest Approach, Environ. Sci. Technol., 51, 6936–6944, https://doi.org/10.1021/acs.est.7b01210, https://pubs.acs.org/doi/10.1021/acs.est.7b01210, 2017.

Hueglin, C., Gehrig, R., Baltensperger, U., Gysel, M., Monn, C., and Vonmont, H.: Chemical characterisation of PM2.5, PM10 and coarse particles at urban, near-city and rural sites in Switzerland, Atmos. Environ., 39, 637–651, https://doi.org/10.1016/j.atmosenv.2004.10.027, 2005.

Hughes, H. E., Morbey, R., Fouillet, A., Caserio-Schönemann, C., Dobney, A., Hughes, T. C., Smith, G. E., and Elliot, A. J.: Retrospective observational study of emergency department syndromic surveillance data during air pollution episodes across London and Paris in 2014, BMJ Open, 8, 1–12, https://doi.org/10.1136/bmjopen-2017-018732, 2018.

Jiang, J., Aksoyoglu, S., El-Haddad, I., Ciarelli, G., Denier van der Gon, H. A. C., Canonaco, F., Gilardoni, S., Paglione, M., Minguillón, M. C., Favez, O., Zhang, Y., Marchand, N., Hao, L., Virtanen, A., Florou, K., Oapos;Dowd, C., Ovadnevaite, J., Baltensperger, U., and Prévôt, A. S. H.: Sources of organic aerosols in Europe: a modeling study using CAMx with modified volatility basis set scheme, Atmos. Chem. Phys., 19, 15 247–15 270, https://doi.org/10.5194/acp-19-15247-2019, https://www.atmos-chem-phys.net/19/15247/2019/, 2019.

Just, A., De Carli, M., Shtein, A., Dorman, M., Lyapustin, A., and Kloog, I.: Correcting Measurement Error in Satellite Aerosol Optical Depth with Machine Learning for Modeling PM2.5 in the Northeastern USA, Remote Sens., 10, 803, https://doi.org/10.3390/rs10050803, http://www.mdpi.com/2072-4292/10/5/803, 2018.

Kiesewetter, G., Borken-Kleefeld, J., Schöpp, W., Heyes, C., Thunis, P., Bessagnet, B., Terrenoire, E., Fagerli, H., Nyiri, A., and Amann, M.: Modelling street level PM10 concentrations across Europe: source apportionment and possible futures, Atmos. Chem. Phys., 15, 1539–1553, https://doi.org/10.5194/acp-15-1539-2015, https://www.atmos-chem-phys.net/15/1539/2015/, 2015.

Klingner, M. and Sähn, E.: Prediction of PM10 concentration on the basis of high resolution weather forecasting, Meteorol. Zeitschrift, 17, 263–272, https://doi.org/10.1127/0941-2948/2008/0288, http://www.schweizerbart.de/papers/metz/detail/17/56689/Prediction_of_PM10_concentration_on_the_basis_of_h?af=crossref, 2008.

Kotthaus, S. and Grimmond, C. S. B.: Atmospheric boundary-layer characteristics from ceilometer measurements. Part 1: A new method to track mixed layer height and classify clouds, Q. J. R. Meteorol. Soc., 144, 1525–1538, https://doi.org/10.1002/qj.3299, 2018a.

Kotthaus, S. and Grimmond, C. S. B.: Atmospheric boundary-layer characteristics from ceilometer measurements. Part 2: Application to London's urban boundary layer, Q. J. R. Meteorol. Soc., 144, 1511–1524, https://doi.org/10.1002/qj.3298, 2018b.

Laborde, M., Crippa, M., Tritscher, T., Jurányi, Z., Decarlo, P. F., Temime-Roussel, B., Marchand, N., Eckhardt, S., Stohl, A., Baltensperger, U., Prévôt, A. S., Weingartner, E., and Gysel, M.: Black carbon physical properties and mixing state in the European megacity Paris, Atmos. Chem. Phys., 13, 5831–5856, https://doi.org/10.5194/acp-13-5831-2013, 2013.

Lelieveld, J., Evans, J. S., Fnais, M., Giannadaki, D., and Pozzer, A.: The contribution of outdoor air pollution sources to premature mortality on a global scale, Nature, 525, 367–371, https://doi.org/10.1038/nature15371, 2015.

Lelieveld, J., Klingmüller, K., Pozzer, A., Pöschl, U., Fnais, M., Daiber, A., and Münzel, T.: Cardiovascular disease burden from ambient air pollution in Europe reassessed using novel hazard ratio functions, Eur. Heart J., 0, 1–7, https://doi.org/10.1093/eurheartj/ehz135, https://academic.oup.com/eurheartj/advance-article/doi/10.1093/eurheartj/ehz135/5372326https://academic.oup.com/eurheartj/article/40/20/1590/5372326, 2019.

Leung, D. M., Tai, A. P. K., Mickley, L. J., Moch, J. M., Van Donkelaar, A., Shen, L., and Martin, R. V.: Synoptic meteorological modes of variability for fine particulate matter (PM 2.5) air quality in major metropolitan regions of China, Atmos. Chem. Phys. Discuss. Chem. Phys. Discuss., started, 1–29, https://doi.org/10.5194/acp-2017-916, 2017.

Li, Y., Zhang, J., Sailor, D. J., and Ban-Weiss, G. A.: Effects of urbanization on regional meteorology and air quality in Southern California, Atmos. Chem. Phys., 19, 4439–4457, https://doi.org/10.5194/acp-19-4439-2019, 2019.

Li, Z., Guo, J., Ding, A., Liao, H., Liu, J., Sun, Y., Wang, T., Xue, H., Zhang, H., and Zhu, B.: Aerosol and boundary-layer interactions and impact on air quality, Natl. Sci. Rev., 4, 810–833, https://doi.org/10.1093/nsr/nwx117, https://academic.oup.com/nsr/article/4/6/810/4191281, 2017.

Liu, Q., Jia, X., Quan, J., Li, J., Li, X., Wu, Y., Chen, D., Wang, Z., and Liu, Y.: New positive feedback mechanism between boundary layer meteorology and secondary aerosol formation during severe haze events, Sci. Rep., 8, 1–8, https://doi.org/10.1038/s41598-018-24366-3, http://dx.doi.org/10.1038/s41598-018-24366-3, 2018.

Lundberg, S. M. and Lee, S.-I.: A Unified Approach to Interpreting Model Predictions, pp. 1–10. arXiv: 1705.07 874, http://arxiv.org/abs/1705.07874, 2017.

Lundberg, S. M., Erion, G. G., and Lee, S.-I.: Consistent Individualized Feature Attribution for Tree Ensembles, pp. 1–9. arXiv:1802.03 888, http://arxiv.org/abs/1802.03888, 2018a.

Lundberg, S. M., Nair, B., Vavilala, M. S., Horibe, M., Eisses, M. J., Adams, T., Liston, D. E., Low, D. K.-W., Newman, S.-F., Kim, J., and Lee, S.-I.: Explainable machine-learning predictions for the prevention of hypoxaemia during surgery, Nat. Biomed. Eng., 2, 749–760, https://doi.org/10.1038/s41551-018-0304-0, http://www.nature.com/articles/s41551-018-0304-0, 2018b.

Lundberg, S. M., Erion, G., Chen, H., DeGrave, A., Prutkin, J. M., Nair, B., Katz, R., Himmelfarb, J., Bansal, N., and Lee, S.-i.: From local explanations to global understanding with explainable AI for trees, Nat. Mach. Intell., 2, 56–67, https://doi.org/10.1038/s42256-019-0138-9, http://dx.doi.org/10.1038/s42256-019-0138-9http://www.nature.com/articles/s42256-019-0138-9, 2020.

McGovern, A., Lagerquist, R., John Gagne, D., Jergensen, G. E., Elmore, K. L., Homeyer, C. R., and Smith, T.: Making the Black Box More Transparent: Understanding the Physical Implications of Machine Learning, Bull. Am. Meteorol. Soc., 100, 2175–2199, https://doi.org/10.1175/BAMS-D-18-0195.1, http://journals.ametsoc.org/doi/10.1175/BAMS-D-18-0195.1, 2019.

Megaritis, A. G., Fountoukis, C., Charalampidis, P. E., Pilinis, C., and Pandis, S. N.: Response of fine particulate matter concentrations to changes of emissions and temperature in Europe, Atmos. Chem. Phys., 13, 3423–3443, https://doi.org/10.5194/acp-13-3423-2013, 2013.

Megaritis, A. G., Fountoukis, C., Charalampidis, P. E., Denier Van Der Gon, H. A., Pilinis, C., and Pandis, S. N.: Linking climate and air quality over Europe: Effects of meteorology on PM2.5 concentrations, Atmos. Chem. Phys., 14, 10 283–10 298, https://doi.org/10.5194/acp-14-10283-2014, 2014.

Ng, N. L., Herndon, S. C., Trimborn, A., Canagaratna, M. R., Croteau, P. L., Onasch, T. B., Sueper, D., Worsnop, D. R., Zhang, Q., Sun, Y. L., and Jayne, J. T.: An Aerosol Chemical Speciation Monitor (ACSM) for routine monitoring of the composition and mass concentrations of ambient aerosol, Aerosol Sci. Technol., 45, 770–784, https://doi.org/10.1080/02786826.2011.560211, 2011.

Paatero, P. and Tapper, U.: Positive matrix factorization: A non-negative factor model with optimal utilization of error estimates of data values, Environmetrics, 5, 111–126, https://doi.org/10.1002/env.3170050203, http://doi.wiley.com/10.1002/env.3170050203, 1994.

Pay, M. T., Jiménez-Guerrero, P., and Baldasano, J. M.: Assessing sensitivity regimes of secondary inorganic aerosol formation in Europe with the CALIOPE-EU modeling system, Atmos. Environ., 51, 146–164, https://doi.org/10.1016/j.atmosenv.2012.01.027, http://dx.doi.org/10.1016/j.atmosenv.2012.01.027, 2012.

Pedregosa, F., Varoquaux, G., Gramfort, A., Michel, V., Thirion, B., Grisel, O., Blondel, M., Müller, A., Nothman, J., Louppe, G., Prettenhofer, P., Weiss, R., Dubourg, V., Vanderplas, J., Passos, A., Cournapeau, D., Brucher, M., Perrot, M., and Duchesnay, É.: Scikit-learn: Machine Learning in Python, J. Mach. Learn. Res., pp. 2825–2830. arXiv: 1201.0490, 2012.

Petäjä, T., Järvi, L., Kerminen, V.-M., Ding, A., Sun, J., Nie, W., Kujansuu, J., Virkkula, A., Yang, X., Fu, C., Zilitinkevich, S., and Kulmala, M.: Enhanced air pollution via aerosol-boundary layer feedback in China, Sci. Rep., 6, 18 998, https://doi.org/10.1038/srep18998, http://www.nature.com/articles/srep18998, 2016.

Petetin, H., Beekmann, M., Sciare, J., Bressi, M., Rosso, A., Sanchez, O., and Ghersi, V.: A novel model evaluation approach focusing on local and advected contributions to urban PM2.5 levels - Application to Paris, France, Geosci. Model Dev., 7, 1483–1505, https://doi.org/10.5194/gmd-7-1483-2014, 2014.

Petit, J. E., Favez, O., Sciare, J., Canonaco, F., Croteau, P., Močnik, G., Jayne, J., Worsnop, D., and Leoz-Garziandia, E.: Submicron aerosol source apportionment of wintertime pollution in Paris, France by double positive matrix factorization (PMF2) using an aerosol chemical

speciation monitor (ACSM) and a multi-wavelength Aethalometer, Atmos. Chem. Phys., 14, 13 773–13 787, https://doi.org/10.5194/acp-14-13773-2014, 2014.

Petit, J.-E., Favez, O., Sciare, J., Crenn, V., Sarda-Estève, R., Bonnaire, N., Močnik, G., Dupont, J.-C., Haeffelin, M., and Leoz-Garziandia, E.: Two years of near real-time chemical composition of submicron aerosols in the region of Paris using an Aerosol Chemical Speciation Monitor (ACSM) and a multi-wavelength Aethalometer, Atmos. Chem. Phys., 15, 2985–3005, https://doi.org/10.5194/acp-15-2985-2015, https://www.atmos-chem-phys.net/15/2985/2015/, 2015.

Petit, J. E., Amodeo, T., Meleux, F., Bessagnet, B., Menut, L., Grenier, D., Pellan, Y., Ockler, A., Rocq, B., Gros, V., Sciare, J., and Favez, O.: Characterising an intense PM pollution episode in March 2015 in France from multi-site approach and near real time data: Climatology, variabilities, geographical origins and model evaluation, Atmos. Environ., 155, 68–84, https://doi.org/10.1016/j.atmosenv.2017.02.012, http://dx.doi.org/10.1016/j.atmosenv.2017.02.012, 2017.

Putaud, J.-P., Raes, F., Van Dingenen, R., Brüggemann, E., Facchini, M.-C., Decesari, S., Fuzzi, S., Gehrig, R., Hüglin, C., Laj, P., Lorbeer, G., Maenhaut, W., Mihalopoulos, N., Müller, K., Querol, X., Rodriguez, S., Schneider, J., Spindler, G., ten Brink, H., Tørseth, K., and Wiedensohler, A.: A European aerosol phenomenology—2: chemical characteristics of particulate matter at kerbside, urban, rural and background sites in Europe, Atmos. Environ., 38, 2579–2595, https://doi.org/10.1016/j.atmosenv.2004.01.041, https://linkinghub.elsevier.com/retrieve/pii/S1352231004000949, 2004.

Radke, L. F., Hobbs, P. V., and Eltgroth, M. W.: Scavenging of aerosol particles by precipitation., J. Appl. Meteorol., 19, 715–722, https://doi.org/10.1175/1520-0450(1980)019<0715:SOAPBP>2.0.CO;2, 1980.

Rengarajan, R., Sudheer, A., and Sarin, M.: Wintertime PM2.5 and PM10 carbonaceous and inorganic constituents from urban site in western India, Atmos. Res., 102, 420–431, https://doi.org/10.1016/j.atmosres.2011.09.005, http://dx.doi.org/10.1016/j.atmosres.2011.09.005https://linkinghub.elsevier.com/retrieve/pii/S0169809511002900, 2011.

Rost, J., Holst, T., Sahn, E., Klingner, M., Anke, K., Ahrens, D., and Mayer, H.: Variability of PM10 concentrations dependent on meteorological conditions, Int. J. Environ. Pollut., 36, 3–18, https://doi.org/10.1504/IJEP.2009.021813, 2009.

Rybarczyk, Y. and Zalakeviciute, R.: Machine learning approaches for outdoor air quality modelling: A systematic review, https://doi.org/10.3390/app8122570, http://www.mdpi.com/2076-3417/8/12/2570, 2018.

Samoli, E., Peng, R., Ramsay, T., Pipikou, M., Touloumi, G., Dominici, F., Burnett, R., Cohen, A., Krewski, D., Samet, J., and Katsouyanni, K.: Acute effects of ambient particulate matter on mortality in Europe and North America: Results from the APHENA study, Environ. Health Perspect., 116, 1480–1486, https://doi.org/10.1289/ehp.11345, 2008.

Samoli, E., Stafoggia, M., Rodopoulou, S., Ostro, B., Declercq, C., Alessandrini, E., Díaz, J., Karanasiou, A., Kelessis, A. G., Le Tertre, A., Pandolfi, P., Randi, G., Scarinzi, C., Zauli-Sajani, S., Katsouyanni, K., and Forastiere, F.: Associations between Fine and Coarse Particles and Mortality in Mediterranean Cities: Results from the MED-PARTICLES Project, Environ. Health Perspect., 121, 932–938, https://doi.org/10.1289/ehp.1206124, https://ehp.niehs.nih.gov/doi/10.1289/ehp.1206124, 2013.

Schäfer, K., Wagner, P., Emeis, S., Jahn, C., Münkel, C., Suppan, P., Ecology, L., and Gmbh, V.: Mixing layer height and air pollution levels in urban area, Proc. SPIE, 8534, 1–10, https://doi.org/10.1117/12.974328, 2012.

Sciare, J., D'Argouges, O., Zhang, Q. J., Sarda-Estève, R., Gaimoz, C., Gros, V., Beekmann, M., and Sanchez, O.: Comparison between simulated and observed chemical composition of fine aerosols in Paris (France) during springtime: Contribution of regional versus continental emissions, Atmos. Chem. Phys., 10, 11 987–12 004, https://doi.org/10.5194/acp-10-11987-2010, 2010.

Shapley, L.: A Value for n-Person Games, in: Contrib. to Theory Games (AM-28), Vol. II, edited by Kuhn, H. W. and Tucker, A. W., vol. 28, pp. 307–318, Princeton University Press, Princeton, https://doi.org/10.1515/9781400881970-018, http://www.degruyter.com/view/books/9781400881970/9781400881970-018/9781400881970-018.xml, 1953.

Srivastava, D., Favez, O., Bonnaire, N., Lucarelli, F., Haeffelin, M., Perraudin, E., Gros, V., Villenave, E., and Albinet, A.: Speciation of organic fractions does matter for aerosol source apportionment. Part 2: Intensive short-term campaign in the Paris area (France), Sci. Total Environ., 634, 267–278, https://doi.org/10.1016/j.scitotenv.2018.03.296, https://doi.org/10.1016/j.scitotenv.2018.03.296https://linkinghub.elsevier.com/retrieve/pii/S0048969718310568, 2018.

Srivastava, D., Favez, O., Petit, J., Zhang, Y., Sofowote, U. M., Hopke, P. K., and Bonnaire, N.: Science of the Total Environment Speciation of organic fractions does matter for aerosol source apportionment . Part 3 : Combining off-line and on-line measurements, Sci. Total Environ., 690, 944–955, https://doi.org/10.1016/j.scitotenv.2019.06.378, https://doi.org/10.1016/j.scitotenv.2019.06.378, 2019.

Stirnberg, R., Cermak, J., Fuchs, J., and Andersen, H.: Mapping and Understanding Patterns of Air Quality Using Satellite Data and Machine Learning, J. Geophys. Res. Atmos., 125, e2019JD031 380, https://doi.org/10.1029/2019JD031380, https://agupubs.onlinelibrary.wiley.com/doi/abs/10.1029/2019JD031380?af=R&utm_source=researcher_app&utm_medium=referral&utm_campaign=RESR_MRKT_Researcher_inbound&sid=researcherhttps://onlinelibrary.wiley.com/doi/abs/10.1029/2019JD031380, 2020.

Su, J. G., Apte, J. S., Lipsitt, J., Garcia-Gonzales, D. A., Beckerman, B. S., de Nazelle, A., Texcalac-Sangrador, J. L., and Jerrett, M.: Populations potentially exposed to traffic-related air pollution in seven world cities, Environ. Int., 78, 82–89, https://doi.org/10.1016/j.envint.2014.12.007, http://dx.doi.org/10.1016/j.envint.2014.12.007, 2015.

Sujatha, P., Mahalakshmi, D., Ramiz, A., Rao, P., and Naidu, C.: Ventilation coefficient and boundary layer height impact on urban air quality, Cogent Environ. Sci., 2, 1–9, https://doi.org/10.1080/23311843.2015.1125284, http://dx.doi.org/10.1080/23311843.2015.1125284https://www.cogentoa.com/article/10.1080/23311843.2015.1125284, 2016.

Wagner, P. and Schäfer, K.: Influence of mixing layer height on air pollutant concentrations in an urban street canyon, Urban Clim., 22, 64–79, https://doi.org/10.1016/j.uclim.2015.11.001, https://doi.org/10.1016/j.uclim.2015.11.001, 2017.

Wang, G., Zhang, R., Gomez, M. E., Yang, L., Zamora, M. L., Hu, M., Lin, Y., Peng, J., Guo, S., Meng, J., Li, J., Cheng, C., Hu, T., Ren, Y., Wang, Y., Gao, J., Cao, J., An, Z., Zhou, W., Li, G., Wang, J., Tian, P., Marrero-Ortiz, W., Secrest, J., Du, Z., Zheng, J., Shang, D., Zeng, L., Shao, M., Wang, W., Huang, Y., Wang, Y., Zhu, Y., Li, Y., Hu, J., Pan, B., Cai, L., Cheng, Y., Ji, Y., Zhang, F., Rosenfeld, D., Liss, P. S., Duce, R. A., Kolb, C. E., and Molina, M. J.: Persistent sulfate formation from London Fog to Chinese haze, Proc. Natl. Acad. Sci. U. S. A., 113, 13 630–13 635, https://doi.org/10.1073/pnas.1616540113, 2016.

Wang, X., Dickinson, R. E., Su, L., Zhou, C., and Wang, K.: PM2.5 Pollution in China and How It Has Been Exacerbated by Terrain and Meteorological Conditions, Bull. Am. Meteorol. Soc., 99, 105–119, https://doi.org/10.1175/BAMS-D-16-0301.1, http://journals.ametsoc.org/doi/10.1175/BAMS-D-16-0301.1, 2018.

Yang, M., Chu, C., Bloom, M. S., Li, S., Chen, G., Heinrich, J., Markevych, I., Knibbs, L. D., Bowatte, G., Dharmage, S. C., Komppula, M., Leskinen, A., Hirvonen, M.-R., Roponen, M., Jalava, P., Wang, S.-Q., Lin, S., Zeng, X.-W., Hu, L.-W., Liu, K.-K., Yang, B.-Y., Chen, W., Guo, Y., and Dong, G.-H.: Is smaller worse? New insights about associations of PM1 and respiratory health in children and adolescents, Environ. Int., 120, 516–524, https://doi.org/10.1016/j.envint.2018.08.027, http://dx.doi.org/10.1016/S2542-5196(17)30095-5https://linkinghub.elsevier.com/retrieve/pii/S2542519617300955https://linkinghub.elsevier.com/retrieve/pii/S0160412018303866, 2018.

Yang, Y. Q., Wang, J. Z., Gong, S. L., Zhang, X. Y., Wang, H., Wang, Y. Q., Wang, J., Li, D., and Guo, J. P.: PLAM - A meteorological pollution index for air quality and its applications in fog-haze forecasts in North China, Atmos. Chem. Phys., 16, 1353–1364, https://doi.org/10.5194/acp-16-1353-2016, 2016.

Zhang, Y., Favez, O., Petit, J. E., Canonaco, F., Truong, F., Bonnaire, N., Crenn, V., Amodeo, T., Prévôt, A. S., Sciare, J., Gros, V., and Albinet, A.: Six-year source apportionment of submicron organic aerosols from near-continuous highly time-resolved measurements at SIRTA (Paris area, France), Atmos. Chem. Phys., 19, 14 755–14 776, https://doi.org/10.5194/acp-19-14755-2019, 2019.